O-GlcNAcylation and oxidation contribute to atrial fibrillation in diabetes by activating CaMKII

Olurotimi O. Mesubi[1*], Adam G. Rokita[2,3], Neha Abrol[1], Yuejin Wu[1], Biyi Chen[2], Qinchuan Wang[1], Jonathan Granger[1], Elizabeth D. Luczak[1], Partha S. Banerjee[4], Lars S. Maier[3], Xander H. Wehrens[5], Joel L. Pomerantz[4,6], Long-Sheng Song[2], Rexford S. Ahima[7], Natasha E. Zachara[4], Gerald W. Hart[4], Mark E. Anderson[1,8,9*].

Affiliations

1. Division of Cardiology, Department of Medicine, The Johns Hopkins University School of Medicine, Baltimore, MD, USA
2. Division of Cardiovascular Medicine and Cardiovascular Research Center, Carver College of Medicine, Iowa City, IA, USA
3. Department of Internal Medicine II, University Hospital Regensburg, Regensburg, Germany
4. Department of Biological Chemistry, The Johns Hopkins University School of Medicine, Baltimore, MD, USA
5. Department of Molecular Physiology & Biophysics, and Medicine (Cardiology), Pediatrics, Center for Space Medicine, Baylor College of Medicine, Houston, TX, USA
6. Institute for Cell Engineering, The Johns Hopkins University School of Medicine, Baltimore, MD, USA
7. Division of Endocrinology, Diabetes and Metabolism, Department of Medicine, The Johns Hopkins University School of Medicine, Baltimore, MD, USA
8. Department of Medicine, The Johns Hopkins University School of Medicine, Baltimore, MD, USA
9. Department of Physiology and the Program in Cellular and Molecular Medicine, The Johns Hopkins University School of Medicine, Baltimore, MD, USA

* Corresponding Authors

Mark E. Anderson
Department of Medicine, The Johns Hopkins School of Medicine
1830 E. Monument Street, Suite 9026
Baltimore, MD 21287
E-mail – mark.anderson@jhmi.edu
Phone – (410) 955-6642
Fax – (410) 614-8510

Olurotimi O. Mesubi
Division of Cardiology, Department of Medicine, The Johns Hopkins School of Medicine
600 N. Wolfe Street, Carnegie 592A
Baltimore, MD, 21287
E-mail – olurotimi.mesubi@jhmi.edu
Phone – (443) 287-8388

Fax – (410) 800-4073

Conflict of interest statement

Dr. Wehrens is co-founder and shareholder of ELEX Biotech, a company aiming to develop RyR2 inhibitor therapeutics. Dr. Hart receives a share of royalty received by the university on sales of the CTD 110.6 antibody, which are managed by The Johns Hopkins University. The other authors report no conflicts of interest.

Abstract

Diabetes mellitus and atrial fibrillation (AF) are major unsolved public health problems, and diabetes is an independent risk factor for AF in patients. However, the mechanism(s) underlying this clinical association is unknown. Elevated protein *O*-GlcNAcylation (OGN) and reactive oxygen species (ROS) are increased in diabetic hearts, and calmodulin kinase II (CaMKII) is a proarrhythmic signal that may be activated by OGN (OGN-CaMKII) and ROS (ox-CaMKII). We induced type 1 (T1D) and type 2 diabetes (T2D) in a portfolio of genetic mouse models capable of dissecting the role of OGN and ROS at CaMKII and the type 2 ryanodine receptor (RyR2), an intracellular Ca^{2+} channel implicated as an important downstream mechanism of CaMKII-mediated arrhythmias. Here we show that T1D and T2D significantly increased AF, similar to observations in patients, and this increase required CaMKII. While T1D and T2D both require ox-CaMKII, they respond differently to loss of OGN-CaMKII. Collectively, our data affirm CaMKII as a critical proarrhythmic signal in diabetic AF, and suggest ROS primarily promotes AF by ox-CaMKII, while OGN promotes AF by diverse mechanisms and targets, including RyR2. However, the proarrhythmic consequences of OGN- and ox-CaMKII differ between T1D and T2D. These results provide new and unanticipated insights into the mechanisms for increased AF in diabetes mellitus, and suggest successful future therapies will need to be different for AF in T1D and T2D.

Keywords

CaMKII, atrial fibrillation, diabetes mellitus, oxidized CaMKII, O-GlcNAcylation, ROS

Abbreviations

Atrial fibrillation - AF
Calcium and calmodulin-dependent protein kinase II – CaMKII
Diabetes mellitus - DM
Diazo-5-oxonorleucine - DON
Methionine sulfoxide reductase A – MsrA
O-GlcNAcase - OGA
O-GlcNAcylation – OGN
O-GlcNAc transferase (OGT)
O-GlcNAcylated CaMKII – OGN-CaMKII
Oxidized CaMKII – ox-CaMKII
Streptozocin – STZ
Type 1 diabetes mellitus – T1D
Type 2 diabetes mellitus – T2D
Type 2 ryanodine receptors – RyR2

Introduction

Atrial fibrillation (AF) and diabetes mellitus (DM) are major, unsolved public health problems (1-3). The disease incidence and prevalence of both conditions are projected to increase significantly in the United States and worldwide in the coming decades (1, 4-7). AF is the most common clinical arrhythmia (8), and it is associated with significant morbidity and mortality (9-12), such as stroke and heart failure. It has become increasingly clear that DM, both type 1 DM (T1D) and type 2 DM (T2D), is an independent risk factor for AF (13-15), and the coexistence of AF and DM results in increased mortality, suffering, and cost (16-18). However, current therapies, such as antiarrhythmic drugs and catheter ablation (19, 20), are inadequate. Improved understanding of the molecular mechanisms connecting DM and AF is an important goal for developing more effective therapies.

DM is characterized by hyperglycemia, elevated levels of reactive oxygen species (ROS) (21, 22) and increased *O*-GlcNAcylation (OGN) (23, 24). OGN is a post-translational protein modification that occurs by attachment of single O-linked N-acetylglucosamine (*O*-GlcNAc) to serines and threonines, resulting in alteration of protein function akin to phosphorylation (25, 26). This dynamic process is controlled exclusively by two enzymes – *O*-GlcNAc transferase (OGT), which catalyzes the addition of *O*-GlcNAc to target residues, and *O*-GlcNAcase (OGA), which catalyzes the removal of *O*-GlcNAc (25, 26). Atrial myocardium from diabetic patients has increased ROS (27, 28) and protein OGN (29). Both ROS and OGN are associated with diabetic cardiomyopathy, and atrial fibrillation (21, 30-34), but it is uncertain if these changes contribute to proarrhythmic molecular pathways favoring atrial fibrillation (21, 35, 36).

The multifunctional calcium and calmodulin-dependent protein kinase II (CaMKII) has emerged as a proarrhythmic signal in AF in the absence of DM (32, 37, 38). Work by us and others, suggests that ROS (39) and OGN (31) can modify the CaMKII regulatory domain, causing CaMKII to become constitutively active, leading to inappropriate Ca^{2+} leak from myocardial type 2 ryanodine receptors (RyR2), triggered action potentials and arrhythmias (31, 32, 40-43). Intriguingly, the ROS (methionines 281/282, ox-CaMKII) and OGN (serine 280, OGN-CaMKII) modified residues of the CaMKII regulatory domain are adjacent, suggesting the hypothesis that CaMKII may integrate these upstream signals – ROS and OGN, which are present in diabetic atrium to favor AF. Despite this, the potential proarrhythmic contributions of ox-CaMKII and OGN-CaMKII have not been directly compared or measured in diabetic cardiomyopathy and diabetic AF.

We performed new experiments to investigate the molecular mechanism(s) by which CaMKII integrates upstream signals from ROS and OGN to promote AF in DM, to understand if CaMKII activation by ROS and/or OGN are critical proarrhythmic mechanisms for diabetic AF, and if the proarrhythmic consequences of CaMKII are similar or different in T1D and T2D. We induced T1D or T2D in a panel of new and established mouse models where ROS and OGN activation of CaMKII was selectively ablated, where ROS and OGN upstream pathways were controlled, and where convergent actions of CaMKII on RyR2 were prevented or mimicked. Our results establish CaMKII as a critical ROS and OGN sensor, and CaMKII activation of RyR2 as an

important proarrhythmic pathway for AF in DM. We found AF in T1D and T2D required ox-CaMKII. However, AF induction in T1D and T2D exhibited different responses to loss of CaMKII activation by OGN, or OGN inhibition by transgenic over-expression of OGA. We discovered that genetic inhibition of OGN by OGA over-expression protected against diabetic AF by CaMKII-dependent and -independent pathways.

Results

Increased AF susceptibility in T1D and T2D is CaMKII-dependent

Excessive CaMKII activity is implicated in non-diabetic AF in patients (32, 37, 38), large animal models (37, 44, 45), and in mice (32, 37, 46). More recently, OGN-CaMKII has been linked to ventricular arrhythmias in diabetic cardiomyopathy (31). In part based on these findings, we hypothesized that CaMKII contributes to hyperglycemia enhanced AF susceptibility. To test this hypothesis, our first approach was to determine the relationship between hyperglycemia and AF in a T1D mouse model. We injected mice with a single dose (185 mg/kg, i.p.) of streptozocin (STZ) to induce T1D (47, 48) (Supplementary Fig 1A). STZ treated (T1D) mice had significantly higher blood glucose (Fig 1A and Supplementary Fig 1B) and reduced body weight (Supplementary Fig 1C) compared with placebo (citrate buffer) treated mice. There was no difference in heart weight indexed for body weight (Supplementary Fig 1D). The T1D mice had slower heart rates (Supplementary Fig 1E), consistent with reports of defective heart rate in diabetic mice (49) and patients (50, 51). Echocardiographic measurements showed impaired left ventricular (LV) systolic function in the T1D mice, compared with non-diabetic littermate controls (Supplementary Fig 1F) without LV hypertrophy or dilation (Supplementary Fig 1G-I), findings similar to patients with diabetic cardiomyopathy (52). The T1D mice showed no evidence of ketoacidosis or renal failure (Supplementary Table 1). Thus, our T1D mice showed marked elevation in glucose, weight loss, and modest, but consistent, impairment in myocardial function, similar to previous reports of diabetic cardiomyopathy (53). To test if this T1D mouse model promotes AF, we performed rapid right atrial burst pacing in anesthetized mice using an established protocol (Fig 1B) (32, 37, 54), with modification of the definition of AF in this study (see Methods section). T1D mice had significantly higher AF compared to non-diabetic controls (Fig 1C). To further probe the effect of hyperglycemia on AF susceptibility, T1D mice were treated with insulin (delivered via osmotic pumps - LinBit) for one week after STZ injection. Insulin treated T1D mice with rescue of hyperglycemia (< 300 mg/dl, Fig 1D) had significantly reduced AF susceptibility compared to insulin treated T1D mice with persistent hyperglycemia (> 300 mg/dl, Fig 1E). These findings, taken together with other reports (14, 15, 55), confirmed that T1D is an AF risk factor in mice, similar to the situation in patients.

To test if CaMKII contributes to hyperglycemia enhanced AF susceptibility, we used mice with myocardial targeted transgenic expression of AC3-I, a CaMKII inhibitory peptide (56). We found that AC3-I mice with T1D were protected from AF compared to wild type (WT) non-diabetic controls (Fig 1C). Despite the reduction in AF, T1D AC3-I mice had similar increases in blood

glucose as the WT T1D mice (Fig 1A). These findings supported the hypothesis that CaMKII is a proarrhythmic signal coupling DM to increased risk of AF.

We considered the T1D model an ideal experimental platform to test the link between hyperglycemia and AF. However, the predominant form of DM in the adult human population affected by AF is T2D (57), a more complex disease characterized by hyperglycemia, impaired insulin secretion and insulin resistance (58). Thus, we next tested AF susceptibility in a T2D mouse model. 5- to 6-week-old male C57BL/6J mice were fed a high-fat diet (HFD) and 5 weeks after initiation of HFD, the mice received daily injections of low dose STZ (40mg/kg/day, i.p.) for three consecutive days (Supplementary Fig 2A). T2D mice had elevated blood glucose (Fig 1F), increased body weight albeit with a slight decrease after STZ injection (Supplementary Fig 2B), no difference in WT levels of fasting insulin (Supplementary Fig 2C), but increased insulin resistance determined by the homeostatic model assessment of insulin resistance (HOMA-IR) (Supplementary Fig 2D). Consistent with the defining features of T2D, our mice showed reduced glucose and insulin tolerance (Supplementary Fig 2E and F) two weeks after low dose STZ injection. T2D mice had significantly higher AF compared to non-diabetic controls (Fig 1G), similar to the findings in the T1D mice and in humans with T2D (14, 15). To determine if CaMKII contributes to AF susceptibility in T2D, we performed right atrial burst pacing in AC3-I T2D mice. Similar to our findings in T1D, AC3-I T2D mice were protected from AF (Fig 1G) compared with non-diabetic controls, and had similar levels of hyperglycemia as WT T2D mice (Fig 1F). Taken together, these findings support the hypothesis that CaMKII is a proarrhythmic signal that is essential for increased risk of AF in validated mouse models of T1D and T2D.

Differential effect of MM281/282 and S280 on AF susceptibility in T1D and T2D

Recent work has provided key insights into the role of ROS (21, 49) and OGN (23, 24, 31) in diabetic cardiomyopathy, including as potential upstream activators of CaMKII, but the role of these signals, and whether they operate independently or together, is untested in vivo. CaMKII is initially activated by binding calcified calmodulin to the calmodulin binding region of the regulatory domain (Fig 2A). After initial activation, ROS and OGN can modify the CaMKII regulatory domain to lock CaMKII into a constitutively active, Ca^{2+} and calmodulin independent conformation that is established to promote arrhythmias and cardiomyopathy (59, 60). ROS activates CaMKII by oxidizing a pair of methionines (M281/282) (39), while OGN activates CaMKII modifying serine 280 (S280) (31) (Fig 2B). The numbering is for CaMKIIδ, the most abundant CaMKII isoform in ventricular myocardium (61-63). We used qRT PCR to measure expression of each CaMKII isoform in human and mouse atrium. We found that, similar to the situation in ventricle, that CaMKIIδ has the highest mRNA expression in human (Supplementary Fig 3A, Supplementary Table 2) and mouse atrium (Supplementary Fig 3B). In addition, CaMKII isoform mRNA expression profile was unchanged in T1D atria compared with WT non-diabetic controls (Supplementary Fig 3C). We measured ROS and OGN in atria from WT T1D, T2D and non-diabetic controls. Consistent with prior animal data and the human data, T1D and T2D atria showed increased ROS (Fig 2C) and OGN (Fig 2D) compared to WT non-diabetic atria. These data are consistent with reports in diabetic patients (27-29), and so potentially set the stage for

increased AF in T1D and T2D due to CaMKII activation by post-translational ROS and OGN modifications.

To determine the role of ox-CaMKII and OGN-CaMKII in hyperglycemia primed-AF, we utilized CaMKIIδ genetically modified (knock-in) mice. Our lab previously generated an ox-CaMKII resistant (MMVV) knock-in mouse (49). These mice are notable for exhibiting resistance to sudden death due to severe bradycardia after myocardial infarction during T1D (49), and are protected from angiotensin II infusion primed AF (32). These findings provided support for the role of ox-CaMKII as a pathological signal in atrial myocardium. OGN activation of CaMKII occurs by modification of a S280 (31), so we developed an OGN-CaMKII resistant (S280A) mouse using CRISPR/Cas9 (64-66) (Supplementary Fig 4A). S280A mice were born in Mendelian ratios, had normal morphology and similar baseline left ventricular (LV) fractional shortening (Supplementary Fig 4B) and LV mass (Supplementary Fig 4C), compared to WT littermate controls. MMVV, S280A, and WT mice have similar total myocardial CaMKII expression (Fig 2E), and resting heart rates (Supplementary Fig 4D). We interpreted these findings, taken together with previous studies on MMVV mice [xyz], to suggest that the S280 and M281/282 sites on CaMKIIδ are dispensable for normal development and basal function.

We induced T1D in MMVV and S280A mice, and performed AF induction studies. T1D MMVV mice were resistant to AF, but T1D S280A mice showed similar AF susceptibility as T1D WT mice (Fig 1C). The WT and S280A T1D mice showed a modest, but consistent decrement in LV fractional shortening compared to non-diabetic counterparts (Supplementary Fig 1F and 4F). In contrast, MMVV mice were resistant to T1D induced LV dysfunction (Supplementary Fig 4F). The T1D MMVVV and S280A mice demonstrated similar increases in blood glucose, and comparable body weight (Supplementary Fig 4G and H). These results suggested that ox-CaMKII at MM281/282, but not OGN-CaMKII at S280, contributed to T1D cardiomyopathy and AF. We next performed AF induction studies in T2D MMVV and S280A mice (Fig 1F). T2D MMVV were resistant to AF, while T2D 280A had a trend towards rescue ($p = 0.07$). We interpret these data to suggest that ox-CaMKII contributes to hyperglycemia primed-AF in both T1D and T2D. In contrast, post-translational modification of the S280 site on CaMKIIδ contributes to AF in T2D but not in T1D.

OGN inhibition has differential effect on AF susceptibility in T1D and T2D

The findings in the S280A mice were unexpected because of published evidence that *O*-GlcNAcylation of CaMKII at S280 in hyperglycemia triggered ventricular arrhythmias (31). However, our studies up to this point did not address the possibility that increased OGN in T1D and T2D (Fig 2D) was proarrhythmic, potentially by actions at targets other than CaMKIIδ. As a first step we asked if the OGN inhibitor Diazo-5-oxonorleucine (DON), a glutamine-fructose amidotransferase antagonist that prevents biosynthesis of UDP-GlcNAc, the *O*-GlcNAc transferase substrate, could reduce or prevent AF in diabetic mice. We administered DON (5mg/kg, i.p. injection) 30 minutes prior to AF induction. DON treatment significantly reduced AF susceptibility in WT T1D mice and S280A T1D mice (Fig 3A). MMVV T1D mice treated with DON had no significant further decrease in AF susceptibility (Fig 3A). These findings suggested

that OGN contributed to diabetic AF in the T1D mouse model, but that this was independent of the S280 site on CaMKIIδ. We next asked if OGN inhibition had antiarrhythmic actions in T2D by treating T2D mice with DON prior to AF induction, as in the earlier T1D studies. Surprisingly, DON treatment was not protective against AF in T2D (Fig 3B). We interpreted these data up to this point to highlight important, but unanticipated differences in the AF mechanisms in T1D and T2D, and to suggest that different future antiarrhythmic therapies may be required for T1D and T2D.

We recognized that the results showing AF suppression by DON need to be interpreted with caution because DON has the potential for off-target effects (67). We developed a transgenic mouse model with myocardial overexpression of OGA (OGA-TG mice) (Fig 3C and 3D), as an orthogonal approach to testing for the therapeutic potential of reducing myocardial OGN in diabetic AF. The OGA-TG mice were born in Mendelian ratios, had normal morphology and similar body weight and blood glucose at baseline compared to WT littermates (Supplementary Fig 5A and B). These mice had normal echocardiographic features including LV fractional shortening, LV mass and LV dimensions (Supplementary Fig 5C – H) and similar resting heart rates (Supplementary Fig 5I) and heart weight indexed for body weight (Supplementary Fig 5J) compared to WT littermates. The OGA-TG mice were protected from increased AF in T1D and T2D compared with WT T1D and T2D mice (Fig 3E and 3G). Both T1D and T2D OGA-TG mice had similar levels of hyperglycemia as T1D and T2D WT mice (Fig 3F and 3H). We interpreted these data to show that OGN signaling likely contributes to AF in T1D and T2D, but S280 is a less important proarrhythmic target in T1D than in T2D.

Attenuation of ROS signaling prevents AF due to hyperglycemia

In contrast to the differential response of T1D and T2D to manipulation of OGN and S280A for AF prevention, data on the role of M281/282 for promoting AF were highly consistent. We next focused on the T1D model, because of its relative simplicity, to test for cellular sources of ROS that were important for ox-CaMKII and AF. Major ROS sources in heart include mitochondria and NADPH oxidases. We used a combination of genetic and pharmacologic approaches to inhibit ROS. Based on our earlier discovery that mitochondrial ROS increases ox-CaMKII in vitro during hyperglycemia (49), we tested if mitochondrial antioxidant therapy could protect against AF in T1D. We found that mice treated with daily injections of MitoTEMPO (1mg/kg, i.p.), a mitochondrial targeted antioxidant (68), for seven days starting one week after STZ injection, were protected from AF in T1D (Fig 4A). In contrast, T1D mice treated with triphenylphosphonium (TPP), the mitochondrial targeting moiety of MitoTEMPO that lacks the anti-oxidant TEMPO, were not protected from AF (Fig 4A). MitoTEMPO and TPP treated mice had similar levels of hyperglycemia (Fig 4B). We confirmed increased mitochondrial ROS in atrial myocytes isolated from T1D using MitoSOX (Fig 4C). NADPH oxidase is another important source of extra-mitochondrial ROS for increasing ox-CaMKII and promoting AF (31, 32, 69). Mice with T1D lacking p47 ($p47^{-/-}$), an important component of myocardial NADPH oxidases (32, 39, 70) were also protected from AF (Fig 4A) and had similar levels of hyperglycemia as WT T1D mice (Fig 4B). Taken together, these data suggested that reduction of ROS signaling either by NADPH oxidase or mitochondrial ROS in the setting of T1D was sufficient to reduce AF risk.

Ox-CaMKII can be reduced by methionine sulfoxide reductase A (MsrA), and mice lacking MsrA (*MsrA*$^{-/-}$) show increased ox-CaMKII (39). In contrast, mice with transgenic myocardial overexpression of MsrA are protected from ox-CaMKII induced cardiomyopathy (71). We found that non-diabetic *MsrA*$^{-/-}$ mice had easily induced AF, similar to WT mice with T1D (Fig 4A), and that MsrA transgenic mice with T1D were protected against AF, similar to non-diabetic WT mice (Fig 4A). The antiarrhythmic responses to mitoTEMPO infusion or MsrA over-expression were not related to effects on hyperglycemia because blood glucose levels were similarly increased in all mice (Fig 4B). We interpreted these findings as an indication that methionine oxidation and ox-CaMKII are elements of conserved proarrhythmic pathway downstream to ROS in T1D.

Ox-CaMKII and OGN enhance triggered activity and RyR2 Ca^{2+} leak

CaMKII is proarrhythmic, in part, by promoting afterdepolarizations (37, 38, 72, 73). Delayed afterdepolarizations (DADs) are observed as membrane potential fluctuations that occur after action potential repolarization (74). In order to test if DADs were increased in atrial myocytes from T1D mice, we rapidly paced isolated atrial myocytes to simulate the model of AF induction by rapid atrial pacing, using patch clamp in current clamp mode (Fig 4D). Atrial myocytes isolated from WT mice with T1D exhibited increased frequency of DADs and spontaneous action potentials compared to non-diabetic controls (Fig 4E). DON reduced DADs and spontaneous action potentials recorded from atrial myocytes from WT mice with T1D. MMVV mice with T1D were resistant to increased DADs and action potentials, and addition of DON further suppressed DADs and action potentials in these cells (Fig 4E). Taken together, we interpret these data to indicate that ox-CaMKII and OGN augment DADs in T1D, a potential cellular mechanism explaining increased propensity for AF in T1D.

Excessive RyR2 Ca^{2+} leak has emerged as a core proarrhythmic mechanism that is activated by CaMKII (75). Furthermore, RyR2 is a candidate arrhythmia target downstream to OGN and ox-CaMKII because DON reduced RyR2 Ca^{2+} leak in cardiomyocytes exposed to hyperglycemia, and suppressed arrhythmias in diabetic rats (31), and MMVV mouse atrial cardiomyocytes were resistant to angiotensin II triggered RyR2 Ca^{2+} leak (32). RyR2 S2814 is a validated CaMKII site (75) and CaMKII catalyzed hyperphosphorylation of S2814 contributes to increased RyR2 Ca^{2+} leak, DADs, and triggered arrhythmias (37, 38, 72, 73). Furthermore, S2814A knock-in mice are resistant to angiotensin II primed AF, a model where ox-CaMKII and RyR2 S2814 are required for proarrhythmia (32). We found increased Ca^{2+} sparks (Fig 5A) in atrial myocytes isolated from WT T1D mice (Fig 5B), but not from MMVV mice (Fig 5C). The T1D increased Ca^{2+} spark frequency was suppressed by DON in WT atrial mycocytes (Fig 5A and B). However, DON did not change the Ca^{2+} spark frequency in MMVV atrial myocytes (Fig 5A and C). We found that the S2814A mice with T1D were resistant to AF (Fig 5D). We used a knock-in RyR2 S2814 phosphomimetic mutation (S2814D) to test if the antiarrhythmic actions of DON observed in T1D mice required this site. We found that AF (Fig 5E) and DADs (Fig 5F) were readily inducible in non-diabetic S2814D mice, and that DON treatment effectively suppressed AF (Fig 5E) and DADs (Fig 5F). We interpreted these data as consistent with the concept that T1D augmented a CaMKII-RyR2 proarrhythmic signaling pathway, but that DON off target actions were

antiarrhythmic and/or that the proarrhythmic competence of the CaMKII-RyR2 pathway could be modified by OGN at yet unknown sites.

Discussion

Differential contribution of S280 and M281/282 to AF in T1D and T2D

Our studies provide new information to understand a mechanism for increased AF in DM. We found increased AF in T1D and T2D mouse models, and that this increased susceptibility to AF was absent in mice with myocardial CaMKII inhibition. Thus, CaMKII appears to be a node connecting upstream signals in T1D and T2D with downstream arrhythmia mechanisms. CaMKII is activated by ROS and OGN, and we confirmed previous observations that ROS and OGN are increased in T1D and T2D. However, we found that OGN contributed to AF in T1D and T2D in different ways. Our studies anticipate the need to perform detailed proteomic studies to compare differences in pathways affected by OGN in T1D and T2D. We found that loss of CaMKIIδ S280, the OGN site known to activate CaMKII (31), was insufficient to prevent AF in T1D, whereas loss of this site protected against AF susceptibility in T2D. However, DON, a competitive inhibitor of the hexosamine biosynthetic pathway that reduces availability of UDP-GlcNAc, the rate limiting substrate for OGN, was effective at suppressing AF in T1D, suggesting that OGN was proarrhythmic in T1D by targeting sites other than CaMKII, and/or that off target actions of DON were antiarrhythmic. Although our current results do not allow us to distinguish between these possibilities, our finding that DON suppressed AF induction in RyR2 S2814D mice confirms DON possesses antiarrhythmic actions beyond the now well recognized CaMKII-RyR2 S2814 pathway. In part, to avoid off target actions of DON we made new transgenic mice with over-expression of OGA. These mice showed resistance to AF in T1D and T2D. Taken together with the lack of resistance to AF in T1D in S280A mice, we interpret the studies in OGA-TG mice to indicate OGN is proarrhythmic in T1D substantially or exclusively due to targets other than CaMKIIδ. In contrast, the shared resistance to AF by S280A and OGA-TG mice in T2D is consistent with CaMKIIδ being a critical proarrhythmic target for OGN in T2D.

In contrast to the different responses of AF in T1D and T2D to manipulation of the OGN pathway, the response to loss of ox-CaMKIIδ was remarkably consistent. The increased susceptibility to AF was similarly suppressed in T1D and T2D in MMVV mice. We interpret these findings to support an important role for CaMKII as a transducer of pathological ROS in AF in the setting of T1D and T2D. Although we only tested the role of candidate ROS sources, and MsrA in T1D, it seems plausible that future studies will confirm that targeted antioxidant interventions, upstream to CaMKII, have the potential to reduce AF risk in T1D and T2D.

OGN is a candidate pathway for antiarrhythmic therapy

At present there are no CaMKII-based therapies available for clinical use, but there is evidence that OGN-based therapeutics are advancing to the clinic (76-78). The potential that such agents

may soon become available is exciting, in part, because they may have broad application, including as antiarrhythmic drugs for AF in patients suffering from DM. If our findings that OGA-TG mice are resistant to AF in T1D and T2D have translational implications for humans, then a possible advantage of OGN-based therapies is that they may be successful in T1D and T2D, likely impacting a diverse array of protein targets. While CaMKII and RyR2 appear to be important targets for pathological actions of OGN, OGN targets myriad proteins and pathways. Transcription factors (26), myofilament proteins (30, 79), and mitochondrial metabolism (80), are affected by OGN, and implicated in myocardial disease. OGN is known to participate in physiological processes (26), and is an essential stress response. Mice lacking OGT show augmented pathological responses to cardiac injury (81). Thus the breadth of OGN substrates, and the requirement for increased OGN to overcome myocardial injury should strike a cautionary note concerning the potential for unintended, off and on target actions with OGN based therapeutics. Availability of drugs, or tool molecules with drug-like properties, will constitute an important step in determining when, how and if OGN therapeutics will be applicable to diabetic patients at risk for AF.

Implications for T1D and T2D

T1D represents approximately 10% of all DM (57), and is defined by core features of insulin deficiency and hyperglycemia. In contrast, T2D is the major type of DM, and is mechanistically more complex and heterogenous than T1D. The major risk factor for T2D is obesity, explaining the increased prevalence of T2D worldwide, and the key characteristics of T2D are insulin resistance and hyperglycemia. We chose validated models of T1D (47, 48) and T2D (82, 83) to test the propensity for AF induction in mice. Our findings add new information by which to compare and contrast the consequences of T1D and T2D in heart. While both models relied on an ox-CaMKII pathway for increased AF, and both models showed increased atrial OGN, T1D and T2D evidenced differential responses to interventions targeting OGN. These differences have the potential to serve as a starting point for future research aiming to interrogate OGN targets, and activity and targeting of OGA and OGT in T1D and T2D.

The shared antiarrhythmic response to loss of CaMKIIδ M281/282, in MMVV knock-in mice, in T1D and T2D coupled with the disparate protection against AF in T2D, but not in T1D by loss of S280, in S280A knock-in mice, has implications for how ROS and OGN are likely to activate CaMKII. Because OGN and ROS are elevated in T1D and T2D, it would seem likely that CaMKII oxidation and OGN occur together as a hybrid, activating post-translational modification. However, this seems less probable given the lack of antiarrhythmic response to S280A mice in T1D but shared antiarrhythmic response measured in T1D and T2D MMVV mice. Although, we currently lack proteomic information to rule in or rule out the possibility that loss of M281/282 impairs S280 OGN, or, reciprocally, that loss of S280 affects the redox status of M281/282, these scenarios would be more plausible if there were conserved protection or concordant lack of protection against AF in MMVV and S280A mice with T1D or T2D. Although important open questions remain, our data identify CaMKII as a unifying cause of AF in diabetes mellitus. These findings, taken together with emergent evidence that CaMKII contributes to multiple aspects of DM, including gluconeogenesis in liver and insulin signaling in skeletal muscle (84-86), suggest

that further study of the role of CaMKII in metabolism and metabolic diseases will be important for improved understanding and treatments.

Methods

Mouse models

Experimental studies were performed on male mice with C57BL/6J background. C57BL/6J and mice lacking a functional NADPH oxidase ($p47^{-/-}$) were purchased from The Jackson Laboratory. Our lab previously described the generation of AC3-I (56) and MsrA (71) transgenic mice. We also previously generated MMVV knock-in mice as previously described (49). S2814A knock-in mice were generated in the Wehrens laboratory (37).
CaMKIIδ-S280A knock-in mice harboring a point mutation in the mouse CaMKIIδ gene to substitute Serine 280 with Alanine (S280A) were generated on a C57BL/6J background using the CRISPR/Cas9 technology. A single-guide RNA (target sequence: 5'-CTGTTGCCTCCATGATGCACAGG-3') was designed to target CaMKIIδ. Synthetic single-stranded DNA for CRISPR-homology repair was designed to harbor mutations including S280A (TCC --> GCG) and NsiI recognition site (ATGCAT). Genotyping of founder mice and generations of offspring was performed initially by both direct sequencing of PCR amplified fragments and PCR genotyping from tail DNA with the following primers: Forward, 5'-AGGAAATGCTTGCCAAAGTAGTG-3'; Reverse, 5'- CCAGCACATACTGCCCTAGC-3'.
Transgenic mice with myocardial targeted overexpression of OGA (Tg OGA mice) were generated on a C57Bl/6J background. Hemagglutinin (HA)-tagged human Meningioma Expressed Antigen 5 (OGlcNAcase, OGA) cDNA (from the Hart lab) was subcloned into the pBS-αMHC-script-hGH vector between the murine αMHC promoter and a human growth hormone polyadeneylation sequences. Purified pronuclear injections of linearized DNA (digested with NotI) were performed in the Johns Hopkins Transgenic Mouse Core Facility and embryos implanted into pseudo-pregnant females to generate C57Bl6/J F1 mice. The F1 pups were screened for insertion of the transgene into the mouse genome by PCR analysis (Figure 3C), using the forward primer, 5'- TGGTCAGGATCTCTAGATTGGT-3' and reverse primer, 5'-TCATAAGTTGCTCAGCTTCCTC-3', producing a product of 850 base pairs.

Diabetic mouse models

Type-1 diabetes (T1D) was induced by a single intraperitoneal (i.p.) injection of streptozotocin (STZ) (185mg/kg, Sigma-Aldrich). After a six hour fast, adult (2 – 4 month old) male mice received an i.p. injection of STZ dissolved in a citrate buffer (citric acid and sodium citrate, pH 4.0) or citrate buffer alone for control mice. These mice were maintained on normal chow diet (NCD) (7913 irradiated NIH-31 modified 6% mouse/rat diet – 15 kg, Envigo, Indianapolis, IN) Blood glucose was checked 7 days later with a glucometer (TRUEresult, Nipro Diagnostics) via tail vein and mice with blood glucose levels ≥ 300mg/dl were considered diabetic. STZ-treated mice that had blood glucose levels < 300mg/dl received a second i.p. injection of STZ after a six-hour fast and blood glucose was checked again 7 days after the repeat injection. If blood

glucose levels at repeat check was ≥ 300mg/dl, the mice were considered diabetic otherwise they were excluded from the study. Blood glucose, echocardiography and electrophysiology study were done 2 weeks after initiation of STZ injections.

To induce a model of type-2 diabetes (T2D), male mice (C57BL/6J and other mouse genotypes used in this study) aged 5 – 6 weeks were maintained on a high-fat diet (HFD) (Rodent diet with 60 kcal% fat – D12492, Research Diets, New Brunswick, NJ). Five weeks following the initiation of HFD, the mice received daily intraperitoneal (i.p.) injections of low dose streptozocin (STZ) (40 mg/kg/day, Sigma-Aldrich) for three consecutive days after a six hour fast on each day. STZ was dissolved in a citrate buffer (citric acid and sodium citrate, pH 4.0). For control mice, age-matched littermates were maintained on NCD (7913 irradiated NIH-31 modified 6% mouse/rat diet – 15 kg, Envigo, Indianapolis, IN) and received daily i.p. injections of citrate buffer for three consecutive days at similar age as the HFD mice. Blood glucose was checked via tail vein using a glucometer (OneTouch Ultra 2 meter) two weeks after STZ or citrate buffer injection. In addition, body weight, insulin tolerance test, glucose tolerance test and echocardiography were performed two weeks after STZ or citrate buffer injections. Insulin resistance was measured using the Homeostatic Model Assessment of Insulin Resistance (HOMA-IR) calculation based on fasting insulin and glucose levels.

Insulin therapy

Exogenous insulin was delivered subcutaneously via sustained release insulin implants – LinBit (LinShin, Toronto, ON, Canada) (87, 88) to T1D mice with blood glucose levels > 300 mg/dl, one week after STZ injection. Two to 4 implants were implanted subcutaneously according to the manufacturer's instructions based on the body weight of the mice.

MitoTEMPO and TPP injections

One week after STZ injection, T1D mice received daily i.p. injections (1mg/kg/day) of MitoTEMPO (2-(2,2,6,6-Tetramethylpiperidin-1-oxyl-4-ylamino)-2-oxoethyl) triphenylphosphonium chloride monohydrate, Enzo Life Sciences, Inc., product number: ALX-430-150-M005) or TPP (Formylmethyl)triphenylphosphonium chloride (2-Oxoethyltriphenylphosphonium chloride) for 7 – 10 days.

DON injections

T1D mice received DON (diazo-5-oxonorleucine, 5 mg/kg, i.p.) (31) dissolved in phosphate-buffered saline 30 minutes – 1 hour prior to induction of anesthesia for electrophysiology study and rapid atrial burst pacing.

Mouse electrophysiology and AF induction

In vivo electrophysiology (EP) studies were performed as previously reported with

some modifications (32, 37, 54) in mice anesthetized with isoflurane (1.5 – 2% for induction and 1 – 2 % for maintenance of anesthesia; Isotec 100 Series Isoflurane Vaporizer; Harvard Apparatus). Mouse core body temperature (monitored by a rectal probe), heart rate and respiratory rate during the procedure were monitored with a heated surgical monitoring system (MouseMonitorTM S, Indus Instruments, USA) and the body temperature was maintained at 37.0 ± 0.5°C. A Millar 1.1F octapolar EP catheter (EPR-800; Millar/ADInstruments, USA) was introduced via the right jugular vein, as previously described [ref], into the right atrium and ventricle for recording intracardiac electrograms. A computer-based data acquisition system (Powerlab 16/30; ADInstruments, USA) simultaneously recorded a 3-lead body surface ECG and up to 4 intracardiac bipolar electrograms (Labchart Pro software, version 7, ADInstruments). Right atrial pacing was achieved by delivering 2-ms current pulses by an external stimulator (STG-3008; Multi Channel Systems). AF inducibility was determined by decremental burst pacing. Burst pacing was started at a cycle length of 40ms, decreasing by 2ms every 2 seconds to a cycle length of 8ms. Burst pacing was performed for a total of five times with an interval of one minute after the end of the previous burst protocol or AF termination. AF was defined as the occurrence of rapid and fragmented atrial electrograms with irregular AV-nodal conduction and ventricular rhythm for at least 1 second. If 1 or more bursts (out of 5) were an AF episode, the mouse was deemed inducible for AF, and non-inducible if there were no AF episodes.

Transthoracic echocardiography

Transthoracic echocardiography was performed in conscious mice using the Sequoia C256 ultrasound system (Malvern, PA) equipped with a 15-MHz linear transducer as previously described (89, 90). Briefly, M-mode echocardiogram was obtained from parasternal views of the left ventricle at the level of the papillary muscles at sweep speed of 200 mm/sec. Left ventricular dimensions were averaged over 3 to 5 beats at physiological heart rates, and left ventricular mass, fractional shortening and ejection fraction were derived. A blinded operator performed image acquisition and analysis.

Human samples

De-identified right atrial tissue samples used for CaMKII isoform expression were obtained from patients undergoing cardiac surgery without atrial fibrillation or diabetes.

Immunoblots

Protein immunodetection by standard western blot techniques was performed. Briefly, mice were sacrificed 2 – 4 weeks after STZ or citrate injection, hearts were

excised and atria were separated and flash frozen in liquid nitrogen and stored at -80°C. Atria were lysed with RIPA buffer containing protease and phosphatase inhibitors. Protein fractionation was performed using Nupage gels (Invitrogen) and transferred to PVDF membranes (Bio-Rad). Blots were incubated with primary antibodies – CaMKII delta (1:1000, catalog ab181052, Abcam), O-GlcNAc (1:2000, custom antibody – CTD 110.6 from the Hart lab), GAPDH (1:10,000, catalog 5174, Cell Signaling); and subsequently with the appropriate HRP-conjugated secondary antibodies – anti-rabbit (1:10,000, catalog 656120, Invitrogen) IgG and anti-mouse (1:10,000, catalog A8786, Sigma-Aldrich) IgM antibodies. Chemiluminescence with ECL reagent (Lumi-Light, Roche) was used for detection. Densitometric analysis was performed using NIH Image J software and band intensity was normalized to the entire Coomassie-stained gel or GAPDH.

Cellular ROS detection

Hearts were removed immediately after sacrifice, cryopreserved and sectioned at 30-µm thickness. As previously described (71), after washing in phosphate-buffered saline, heart tissue was pre-incubated with DHE for 30 minutes at 37°C and washed. Fluorescence was detected with a laser scanning confocal microscope (Zeiss 510, 40x oil immersion lens) with excitation at 488 nm and detection at 585 nm. The same scanning parameters were applied to all samples and image analysis was done using NIH Image J software.

Mitochondrial ROS detection

Isolated cardiomyocytes were incubated for 30 minutes with 5µM MitoSOX Red (ThermoFischer Scientific) and 100nM Mitotracker Green (ThermoFischer Scientific). After washing the cells, fluorescence was detected with a laser scanning confocal microscope (Zeiss 510, 40x oil immersion lens). MitoSOX Red (excitation at 510 nm and emission at 580 nm), MitoTracker Green (excitation at 490 nm and emission at 516 nm). Fluorescence was assessed from at least 20 cells in the cell suspension from each mouse. The same scanning parameters were applied to all samples and image analysis was done using NIH Image J software.

Quantitative PCR for CaMKII isoforms

Total RNA from mouse and human atrial tissue was extracted using Trizol reagent (Invitrogen) according to the manufacturer's instructions. After first strand cDNA synthesis, messenger RNA expression was analyzed by quantitative real-time polymerase chain reaction on a BioRad CFX machine using pre-validated primers with SsoAdvanced Universal SYBR Green Supermix (Bio-Rad). GAPDH gene expression was used as the reference gene and the specificity of the assay was confirmed by melting curve analysis.

Calcium imaging in isolated atrial myocytes

Calcium imaging of isolated atrial myocytes was performed as described previously (32, 91).

Isolated atrial myocyte action potential recording

Voltage clamp studies using the perforated patch configuration on isolated atrial myocytes were performed as described previously to record single cell action potentials (32, 92).

Statistics

All results are expressed as mean ± s.e.m. for continuous variables or percentages for dichotomous variables. For continuous variables, statistical analyses was performed using an unpaired Student's t-test (2-tailed – for 2 groups) or one-way ANOVA followed by Tukey's post-hoc multiple comparisons (for ≥ 3 groups). For dichotomous variables, statistical analyses were performed using Fischer's exact test (2-tailed for 2 groups) or a Chi-square test with appropriate correction for post-hoc multiple comparisons (for ≥ 3 groups). A p-value of < 0.05 was considered statistically significant.

Study approval

The Johns Hopkins University animal care and use committee approved all animal experimental protocols. For human samples, the local institutional review board of the Goettingen University approved all human procedures and each patient gave written informed consent.

Author Contributions

MEA, OOM and AGR conceived the project, GWH, PSB, RSA, NEZ and EDL contributed important input for planning the studies, and MEA and OOM wrote the manuscript. NA and JLP developed the S280A mouse. XHW provided the S2814A mouse. BC, L-SS, and YW performed cellular electrophysiological and Ca^{2+} measurement studies. LSM and AGR provided human specimens. EDL, NEZ and PSB performed CaMKII assays and OGN studies. All authors edited and approved the final manuscript.

Acknowledgements

We are grateful to Jinying Yang for her assistance in maintaining mouse colonies. We are also grateful to Djahida Bedja for performing the mouse echocardiograms. We thank Chip Hawkins and the Johns Hopkins University School of Medicine Transgenic Core Laboratory for their technical expertise in generating transgenic mice. We also thank Teresa Ruggle who produced the artwork.

Funding

This work was funded in part by the US National Institutes of Health (NIH) grants [R35 HL140034 to M.E.A.; R01-HL089598, R01-HL091947, R01-HL117641to X.H.W.; and T32-HL007227 to O.O.M.)] and the Foundation Leducq [Career Development Award to A.G.R.]. In addition, this work was supported by an American Heart Association (AHA) collaborative science award (17CSA33610107 to M.E.A and G.W.H.), and an AHA grant (13EIA14560061 to X.H.W.). L.S.M. was supported by the Deutsche Forschungsgemeinschaft Ma 1982/5-1. A Synergy Award from Johns Hopkins University to M.E.A. and G.W.H. and the Johns Hopkins Medicine Discovery Fund also made this work possible.

References

1. Chugh SS, Havmoeller R, Narayanan K, Singh D, Rienstra M, Benjamin EJ, Gillum RF, Kim YH, McAnulty JH, Jr., Zheng ZJ, et al. Worldwide epidemiology of atrial fibrillation: a Global Burden of Disease 2010 Study. *Circulation.* 2014;129(8):837-47.
2. King H, Aubert RE, and Herman WH. Global burden of diabetes, 1995-2025: prevalence, numerical estimates, and projections. *Diabetes Care.* 1998;21(9):1414-31.
3. Centers for Disease Control and Prevention. National Diabetes Statistics Report: Estimates of Diabetes and Its Burden in the United States A, GA: U.S. Department of Health and Human Services; 2014.; 2014.
4. Miyasaka Y, Barnes ME, Gersh BJ, Cha SS, Bailey KR, Abhayaratna WP, Seward JB, and Tsang TS. Secular trends in incidence of atrial fibrillation in Olmsted County, Minnesota, 1980 to 2000, and implications on the projections for future prevalence. *Circulation.* 2006;114(2):119-25.
5. Naccarelli GV, Varker H, Lin J, and Schulman KL. Increasing prevalence of atrial fibrillation and flutter in the United States. *Am J Cardiol.* 2009;104(11):1534-9.
6. Collaboration NCDRF. Worldwide trends in diabetes since 1980: a pooled analysis of 751 population-based studies with 4.4 million participants. *Lancet.* 2016;387(10027):1513-30.
7. Wild S, Roglic G, Green A, Sicree R, and King H. Global prevalence of diabetes: estimates for the year 2000 and projections for 2030. *Diabetes Care.* 2004;27(5):1047-53.
8. Fuster V, Ryden LE, Cannom DS, Crijns HJ, Curtis AB, Ellenbogen KA, Halperin JL, Le Heuzey JY, Kay GN, Lowe JE, et al. ACC/AHA/ESC 2006 Guidelines for the Management of Patients with Atrial Fibrillation: a report of the American College of Cardiology/American Heart Association Task Force on Practice Guidelines and the European Society of Cardiology Committee for Practice Guidelines (Writing Committee to Revise the 2001 Guidelines for the Management of Patients With Atrial Fibrillation): developed in collaboration with the European Heart Rhythm Association and the Heart Rhythm Society. *Circulation.* 2006;114(7):e257-354.
9. Go AS, Hylek EM, Phillips KA, Chang Y, Henault LE, Selby JV, and Singer DE. Prevalence of diagnosed atrial fibrillation in adults: national implications for rhythm management and stroke prevention: the AnTicoagulation and Risk Factors in Atrial Fibrillation (ATRIA) Study. *JAMA.* 2001;285(18):2370-5.

10. Benjamin EJ, Wolf PA, D'Agostino RB, Silbershatz H, Kannel WB, and Levy D. Impact of atrial fibrillation on the risk of death: the Framingham Heart Study. *Circulation.* 1998;98(10):946-52.
11. Thrall G, Lane D, Carroll D, and Lip GY. Quality of life in patients with atrial fibrillation: a systematic review. *Am J Med.* 2006;119(5):448 e1-19.
12. Odutayo A, Wong CX, Hsiao AJ, Hopewell S, Altman DG, and Emdin CA. Atrial fibrillation and risks of cardiovascular disease, renal disease, and death: systematic review and meta-analysis. *BMJ.* 2016;354(i4482.
13. Dahlqvist S, Rosengren A, Gudbjornsdottir S, Pivodic A, Wedel H, Kosiborod M, Svensson AM, and Lind M. Risk of atrial fibrillation in people with type 1 diabetes compared with matched controls from the general population: a prospective case-control study. *Lancet Diabetes Endocrinol.* 2017;5(10):799-807.
14. Kannel WB, Abbott RD, Savage DD, and McNamara PM. Epidemiologic features of chronic atrial fibrillation: the Framingham study. *N Engl J Med.* 1982;306(17):1018-22.
15. Benjamin EJ, Levy D, Vaziri SM, D'Agostino RB, Belanger AJ, and Wolf PA. Independent risk factors for atrial fibrillation in a population-based cohort. The Framingham Heart Study. *JAMA.* 1994;271(11):840-4.
16. Aksnes TA, Schmieder RE, Kjeldsen SE, Ghani S, Hua TA, and Julius S. Impact of new-onset diabetes mellitus on development of atrial fibrillation and heart failure in high-risk hypertension (from the VALUE Trial). *Am J Cardiol.* 2008;101(5):634-8.
17. DeVore AD, Hellkamp AS, Becker RC, Berkowitz SD, Breithardt G, Hacke W, Halperin JL, Hankey GJ, Mahaffey KW, Nessel CC, et al. Hospitalizations in patients with atrial fibrillation: an analysis from ROCKET AF. *Europace.* 2016;18(8):1135-42.
18. Du X, Ninomiya T, de Galan B, Abadir E, Chalmers J, Pillai A, Woodward M, Cooper M, Harrap S, Hamet P, et al. Risks of cardiovascular events and effects of routine blood pressure lowering among patients with type 2 diabetes and atrial fibrillation: results of the ADVANCE study. *Eur Heart J.* 2009;30(9):1128-35.
19. Camm AJ, Lip GY, De Caterina R, Savelieva I, Atar D, Hohnloser SH, Hindricks G, Kirchhof P, and Guidelines ESCCfP. 2012 focused update of the ESC Guidelines for the management of atrial fibrillation: an update of the 2010 ESC Guidelines for the management of atrial fibrillation. Developed with the special contribution of the European Heart Rhythm Association. *Eur Heart J.* 2012;33(21):2719-47.
20. Morillo CA, Verma A, Connolly SJ, Kuck KH, Nair GM, Champagne J, Sterns LD, Beresh H, Healey JS, Natale A, et al. Radiofrequency ablation vs antiarrhythmic drugs as first-line treatment of paroxysmal atrial fibrillation (RAAFT-2): a randomized trial. *JAMA.* 2014;311(7):692-700.
21. Shah MS, and Brownlee M. Molecular and Cellular Mechanisms of Cardiovascular Disorders in Diabetes. *Circ Res.* 2016;118(11):1808-29.
22. Faria A, and Persaud SJ. Cardiac oxidative stress in diabetes: Mechanisms and therapeutic potential. *Pharmacol Ther.* 2016.
23. Dassanayaka S, and Jones SP. O-GlcNAc and the cardiovascular system. *Pharmacol Ther.* 2014;142(1):62-71.
24. Fricovsky ES, Suarez J, Ihm SH, Scott BT, Suarez-Ramirez JA, Banerjee I, Torres-Gonzalez M, Wang H, Ellrott I, Maya-Ramos L, et al. Excess protein O-GlcNAcylation and the progression of diabetic cardiomyopathy. *Am J Physiol Regul Integr Comp Physiol.* 2012;303(7):R689-99.

25. Hart GW, Housley MP, and Slawson C. Cycling of O-linked beta-N-acetylglucosamine on nucleocytoplasmic proteins. *Nature.* 2007;446(7139):1017-22.
26. Hart GW, Slawson C, Ramirez-Correa G, and Lagerlof O. Cross talk between O-GlcNAcylation and phosphorylation: roles in signaling, transcription, and chronic disease. *Annu Rev Biochem.* 2011;80(825-58.
27. Mihm MJ, Yu F, Carnes CA, Reiser PJ, McCarthy PM, Van Wagoner DR, and Bauer JA. Impaired myofibrillar energetics and oxidative injury during human atrial fibrillation. *Circulation.* 2001;104(2):174-80.
28. Anderson EJ, Kypson AP, Rodriguez E, Anderson CA, Lehr EJ, and Neufer PD. Substrate-specific derangements in mitochondrial metabolism and redox balance in the atrium of the type 2 diabetic human heart. *J Am Coll Cardiol.* 2009;54(20):1891-8.
29. Jensen RV, Zachara NE, Nielsen PH, Kimose HH, Kristiansen SB, and Botker HE. Impact of O-GlcNAc on cardioprotection by remote ischaemic preconditioning in non-diabetic and diabetic patients. *Cardiovasc Res.* 2013;97(2):369-78.
30. Ramirez-Correa GA, Ma J, Slawson C, Zeidan Q, Lugo-Fagundo NS, Xu M, Shen X, Gao WD, Caceres V, Chakir K, et al. Removal of Abnormal Myofilament O-GlcNAcylation Restores Ca2+ Sensitivity in Diabetic Cardiac Muscle. *Diabetes.* 2015;64(10):3573-87.
31. Erickson JR, Pereira L, Wang L, Han G, Ferguson A, Dao K, Copeland RJ, Despa F, Hart GW, Ripplinger CM, et al. Diabetic hyperglycaemia activates CaMKII and arrhythmias by O-linked glycosylation. *Nature.* 2013;502(7471):372-6.
32. Purohit A, Rokita AG, Guan X, Chen B, Koval OM, Voigt N, Neef S, Sowa T, Gao Z, Luczak ED, et al. Oxidized Ca(2+)/calmodulin-dependent protein kinase II triggers atrial fibrillation. *Circulation.* 2013;128(16):1748-57.
33. Kronlage M, Dewenter M, Grosso J, Fleming T, Oehl U, Lehmann LH, Falcao-Pires I, Leite-Moreira AF, Volk N, Grone HJ, et al. O-GlcNAcylation of Histone Deacetylase 4 Protects the Diabetic Heart From Failure. *Circulation.* 2019;140(7):580-94.
34. Yoo S, Aistrup G, Shiferaw Y, Ng J, Mohler PJ, Hund TJ, Waugh T, Browne S, Gussak G, Gilani M, et al. Oxidative stress creates a unique, CaMKII-mediated substrate for atrial fibrillation in heart failure. *JCI Insight.* 2018;3(21).
35. Doenst T, Nguyen TD, and Abel ED. Cardiac metabolism in heart failure: implications beyond ATP production. *Circ Res.* 2013;113(6):709-24.
36. Jia G, DeMarco VG, and Sowers JR. Insulin resistance and hyperinsulinaemia in diabetic cardiomyopathy. *Nat Rev Endocrinol.* 2016;12(3):144-53.
37. Chelu MG, Sarma S, Sood S, Wang S, van Oort RJ, Skapura DG, Li N, Santonastasi M, Muller FU, Schmitz W, et al. Calmodulin kinase II-mediated sarcoplasmic reticulum Ca2+ leak promotes atrial fibrillation in mice. *J Clin Invest.* 2009;119(7):1940-51.
38. Neef S, Dybkova N, Sossalla S, Ort KR, Fluschnik N, Neumann K, Seipelt R, Schondube FA, Hasenfuss G, and Maier LS. CaMKII-dependent diastolic SR Ca2+ leak and elevated diastolic Ca2+ levels in right atrial myocardium of patients with atrial fibrillation. *Circ Res.* 2010;106(6):1134-44.
39. Erickson JR, Joiner ML, Guan X, Kutschke W, Yang J, Oddis CV, Bartlett RK, Lowe JS, O'Donnell SE, Aykin-Burns N, et al. A dynamic pathway for calcium-independent activation of CaMKII by methionine oxidation. *Cell.* 2008;133(3):462-74.

40. Wu Y, Roden DM, and Anderson ME. Calmodulin kinase inhibition prevents development of the arrhythmogenic transient inward current. *Circ Res.* 1999;84(8):906-12.
41. Sommese L, Valverde CA, Blanco P, Castro MC, Rueda OV, Kaetzel M, Dedman J, Anderson ME, Mattiazzi A, and Palomeque J. Ryanodine receptor phosphorylation by CaMKII promotes spontaneous Ca(2+) release events in a rodent model of early stage diabetes: The arrhythmogenic substrate. *Int J Cardiol.* 2016;202(394-406.
42. Wagner S, Ruff HM, Weber SL, Bellmann S, Sowa T, Schulte T, Anderson ME, Grandi E, Bers DM, Backs J, et al. Reactive oxygen species-activated Ca/calmodulin kinase IIdelta is required for late I(Na) augmentation leading to cellular Na and Ca overload. *Circ Res.* 2011;108(5):555-65.
43. Gonano LA, Sepulveda M, Rico Y, Kaetzel M, Valverde CA, Dedman J, Mattiazzi A, and Vila Petroff M. Calcium-calmodulin kinase II mediates digitalis-induced arrhythmias. *Circ Arrhythm Electrophysiol.* 2011;4(6):947-57.
44. Greiser M, Neuberger HR, Harks E, El-Armouche A, Boknik P, de Haan S, Verheyen F, Verheule S, Schmitz W, Ravens U, et al. Distinct contractile and molecular differences between two goat models of atrial dysfunction: AV block-induced atrial dilatation and atrial fibrillation. *J Mol Cell Cardiol.* 2009;46(3):385-94.
45. Wakili R, Yeh YH, Yan Qi X, Greiser M, Chartier D, Nishida K, Maguy A, Villeneuve LR, Boknik P, Voigt N, et al. Multiple potential molecular contributors to atrial hypocontractility caused by atrial tachycardia remodeling in dogs. *Circ Arrhythm Electrophysiol.* 2010;3(5):530-41.
46. Fischer TH, Herting J, Mason FE, Hartmann N, Watanabe S, Nikolaev VO, Sprenger JU, Fan P, Yao L, Popov AF, et al. Late INa increases diastolic SR-Ca2+-leak in atrial myocardium by activating PKA and CaMKII. *Cardiovasc Res.* 2015;107(1):184-96.
47. Rossini AA, Like AA, Chick WL, Appel MC, and Cahill GF, Jr. Studies of streptozotocin-induced insulitis and diabetes. *Proc Natl Acad Sci U S A.* 1977;74(6):2485-9.
48. Tomlinson KC, Gardiner SM, Hebden RA, and Bennett T. Functional consequences of streptozotocin-induced diabetes mellitus, with particular reference to the cardiovascular system. *Pharmacol Rev.* 1992;44(1):103-50.
49. Luo M, Guan X, Luczak ED, Lang D, Kutschke W, Gao Z, Yang J, Glynn P, Sossalla S, Swaminathan PD, et al. Diabetes increases mortality after myocardial infarction by oxidizing CaMKII. *J Clin Invest.* 2013;123(3):1262-74.
50. Hasslacher C, and Wahl P. Diabetes prevalence in patients with bradycardiac arrhythmias. *Acta Diabetol Lat.* 1977;14(5-6):229-34.
51. Abenavoli T, Rubler S, Fisher VJ, Axelrod HI, and Zuckerman KP. Exercise testing with myocardial scintigraphy in asymptomatic diabetic males. *Circulation.* 1981;63(1):54-64.
52. Fang ZY, Prins JB, and Marwick TH. Diabetic cardiomyopathy: evidence, mechanisms, and therapeutic implications. *Endocr Rev.* 2004;25(4):543-67.
53. Hsueh W, Abel ED, Breslow JL, Maeda N, Davis RC, Fisher EA, Dansky H, McClain DA, McIndoe R, Wassef MK, et al. Recipes for creating animal models of diabetic cardiovascular disease. *Circ Res.* 2007;100(10):1415-27.
54. Verheule S, Sato T, Everett Tt, Engle SK, Otten D, Rubart-von der Lohe M, Nakajima HO, Nakajima H, Field LJ, and Olgin JE. Increased vulnerability to atrial fibrillation in

transgenic mice with selective atrial fibrosis caused by overexpression of TGF-beta1. *Circ Res.* 2004;94(11):1458-65.

55. Yi F, Ling TY, Lu T, Wang XL, Li J, Claycomb WC, Shen WK, and Lee HC. Down-regulation of the small conductance calcium-activated potassium channels in diabetic mouse atria. *J Biol Chem.* 2015;290(11):7016-26.
56. Zhang R, Khoo MS, Wu Y, Yang Y, Grueter CE, Ni G, Price EE, Jr., Thiel W, Guatimosim S, Song LS, et al. Calmodulin kinase II inhibition protects against structural heart disease. *Nat Med.* 2005;11(4):409-17.
57. Bullard KM, Cowie CC, Lessem SE, Saydah SH, Menke A, Geiss LS, Orchard TJ, Rolka DB, and Imperatore G. Prevalence of Diagnosed Diabetes in Adults by Diabetes Type - United States, 2016. *MMWR Morb Mortal Wkly Rep.* 2018;67(12):359-61.
58. Lillioja S, Mott DM, Spraul M, Ferraro R, Foley JE, Ravussin E, Knowler WC, Bennett PH, and Bogardus C. Insulin resistance and insulin secretory dysfunction as precursors of non-insulin-dependent diabetes mellitus. Prospective studies of Pima Indians. *N Engl J Med.* 1993;329(27):1988-92.
59. Anderson ME, Brown JH, and Bers DM. CaMKII in myocardial hypertrophy and heart failure. *J Mol Cell Cardiol.* 2011;51(4):468-73.
60. Swaminathan PD, Purohit A, Hund TJ, and Anderson ME. Calmodulin-dependent protein kinase II: linking heart failure and arrhythmias. *Circ Res.* 2012;110(12):1661-77.
61. Hoch B, Meyer R, Hetzer R, Krause EG, and Karczewski P. Identification and expression of delta-isoforms of the multifunctional Ca2+/calmodulin-dependent protein kinase in failing and nonfailing human myocardium. *Circ Res.* 1999;84(6):713-21.
62. Colomer JM, Mao L, Rockman HA, and Means AR. Pressure overload selectively up-regulates Ca2+/calmodulin-dependent protein kinase II in vivo. *Mol Endocrinol.* 2003;17(2):183-92.
63. Kreusser MM, Lehmann LH, Keranov S, Hoting MO, Oehl U, Kohlhaas M, Reil JC, Neumann K, Schneider MD, Hill JA, et al. Cardiac CaM Kinase II genes delta and gamma contribute to adverse remodeling but redundantly inhibit calcineurin-induced myocardial hypertrophy. *Circulation.* 2014;130(15):1262-73.
64. Hamblet CE, Makowski SL, Tritapoe JM, and Pomerantz JL. NK Cell Maturation and Cytotoxicity Are Controlled by the Intramembrane Aspartyl Protease SPPL3. *J Immunol.* 2016;196(6):2614-26.
65. Wang H, Yang H, Shivalila CS, Dawlaty MM, Cheng AW, Zhang F, and Jaenisch R. One-step generation of mice carrying mutations in multiple genes by CRISPR/Cas-mediated genome engineering. *Cell.* 2013;153(4):910-8.
66. Yang H, Wang H, and Jaenisch R. Generating genetically modified mice using CRISPR/Cas-mediated genome engineering. *Nat Protoc.* 2014;9(8):1956-68.
67. Lemberg KM, Vornov JJ, Rais R, and Slusher BS. We're Not "DON" Yet: Optimal Dosing and Prodrug Delivery of 6-Diazo-5-oxo-L-norleucine. *Mol Cancer Ther.* 2018;17(9):1824-32.
68. Murphy MP, and Smith RA. Targeting antioxidants to mitochondria by conjugation to lipophilic cations. *Annu Rev Pharmacol Toxicol.* 2007;47(629-56.
69. Reilly SN, Jayaram R, Nahar K, Antoniades C, Verheule S, Channon KM, Alp NJ, Schotten U, and Casadei B. Atrial sources of reactive oxygen species vary with the duration and substrate of atrial fibrillation: implications for the antiarrhythmic effect of statins. *Circulation.* 2011;124(10):1107-17.

70. Jackson SH, Gallin JI, and Holland SM. The p47phox mouse knock-out model of chronic granulomatous disease. *J Exp Med.* 1995;182(3):751-8.
71. He BJ, Joiner ML, Singh MV, Luczak ED, Swaminathan PD, Koval OM, Kutschke W, Allamargot C, Yang J, Guan X, et al. Oxidation of CaMKII determines the cardiotoxic effects of aldosterone. *Nat Med.* 2011;17(12):1610-8.
72. Li N, Wang T, Wang W, Cutler MJ, Wang Q, Voigt N, Rosenbaum DS, Dobrev D, and Wehrens XH. Inhibition of CaMKII phosphorylation of RyR2 prevents induction of atrial fibrillation in FKBP12.6 knockout mice. *Circ Res.* 2012;110(3):465-70.
73. van Oort RJ, McCauley MD, Dixit SS, Pereira L, Yang Y, Respress JL, Wang Q, De Almeida AC, Skapura DG, Anderson ME, et al. Ryanodine receptor phosphorylation by calcium/calmodulin-dependent protein kinase II promotes life-threatening ventricular arrhythmias in mice with heart failure. *Circulation.* 2010;122(25):2669-79.
74. Schlotthauer K, and Bers DM. Sarcoplasmic reticulum Ca(2+) release causes myocyte depolarization. Underlying mechanism and threshold for triggered action potentials. *Circ Res.* 2000;87(9):774-80.
75. Wehrens XH, Lehnart SE, Reiken SR, and Marks AR. Ca2+/calmodulin-dependent protein kinase II phosphorylation regulates the cardiac ryanodine receptor. *Circ Res.* 2004;94(6):e61-70.
76. Selnick HG, Hess JF, Tang C, Liu K, Schachter JB, Ballard JE, Marcus J, Klein DJ, Wang X, Pearson M, et al. Discovery of MK-8719, a Potent O-GlcNAcase Inhibitor as a Potential Treatment for Tauopathies. *J Med Chem.* 2019;62(22):10062-97.
77. Abdel-Magid AF. Inhibition of O-GlcNAcase (OGA): A Potential Therapeutic Target to Treat Alzheimer's Disease. *ACS Med Chem Lett.* 2014;5(12):1270-1.
78. Yuzwa SA, Shan X, Jones BA, Zhao G, Woodward ML, Li X, Zhu Y, McEachern EJ, Silverman MA, Watson NV, et al. Pharmacological inhibition of O-GlcNAcase (OGA) prevents cognitive decline and amyloid plaque formation in bigenic tau/APP mutant mice. *Mol Neurodegener.* 2014;9(42.
79. Ramirez-Correa GA, Jin W, Wang Z, Zhong X, Gao WD, Dias WB, Vecoli C, Hart GW, and Murphy AM. O-linked GlcNAc modification of cardiac myofilament proteins: a novel regulator of myocardial contractile function. *Circ Res.* 2008;103(12):1354-8.
80. Banerjee PS, Ma J, and Hart GW. Diabetes-associated dysregulation of O-GlcNAcylation in rat cardiac mitochondria. *Proc Natl Acad Sci U S A.* 2015;112(19):6050-5.
81. Watson LJ, Facundo HT, Ngoh GA, Ameen M, Brainard RE, Lemma KM, Long BW, Prabhu SD, Xuan YT, and Jones SP. O-linked beta-N-acetylglucosamine transferase is indispensable in the failing heart. *Proc Natl Acad Sci U S A.* 2010;107(41):17797-802.
82. Lv L, Zhang J, Zhang L, Xue G, Wang P, Meng Q, and Liang W. Essential role of Pin1 via STAT3 signalling and mitochondria-dependent pathways in restenosis in type 2 diabetes. *J Cell Mol Med.* 2013;17(8):989-1005.
83. Zhan YY, Chen Y, Zhang Q, Zhuang JJ, Tian M, Chen HZ, Zhang LR, Zhang HK, He JP, Wang WJ, et al. The orphan nuclear receptor Nur77 regulates LKB1 localization and activates AMPK. *Nat Chem Biol.* 2012;8(11):897-904.
84. Ozcan L, Wong CC, Li G, Xu T, Pajvani U, Park SK, Wronska A, Chen BX, Marks AR, Fukamizu A, et al. Calcium signaling through CaMKII regulates hepatic glucose production in fasting and obesity. *Cell Metab.* 2012;15(5):739-51.

85. Ozcan L, Cristina de Souza J, Harari AA, Backs J, Olson EN, and Tabas I. Activation of calcium/calmodulin-dependent protein kinase II in obesity mediates suppression of hepatic insulin signaling. *Cell Metab.* 2013;18(6):803-15.
86. Ozcan L, Xu X, Deng SX, Ghorpade DS, Thomas T, Cremers S, Hubbard B, Serrano-Wu MH, Gaestel M, Landry DW, et al. Treatment of Obese Insulin-Resistant Mice With an Allosteric MAPKAPK2/3 Inhibitor Lowers Blood Glucose and Improves Insulin Sensitivity. *Diabetes.* 2015;64(10):3396-405.
87. Wang PY. Palmitic acid as an excipient in implants for sustained release of insulin. *Biomaterials.* 1991;12(1):57-62.
88. Ohzato H, Porter J, Monaco AP, Montana E, and Maki T. Minimum number of islets required to maintain euglycemia and their reduced immunogenicity after transplantation into diabetic mice. *Transplantation.* 1993;56(2):270-4.
89. Olson LE, Bedja D, Alvey SJ, Cardounel AJ, Gabrielson KL, and Reeves RH. Protection from doxorubicin-induced cardiac toxicity in mice with a null allele of carbonyl reductase 1. *Cancer Res.* 2003;63(20):6602-6.
90. Wei H, Bedja D, Koitabashi N, Xing D, Chen J, Fox-Talbot K, Rouf R, Chen S, Steenbergen C, Harmon JW, et al. Endothelial expression of hypoxia-inducible factor 1 protects the murine heart and aorta from pressure overload by suppression of TGF-beta signaling. *Proc Natl Acad Sci U S A.* 2012;109(14):E841-50.
91. Guatimosim S, Guatimosim C, and Song LS. Imaging calcium sparks in cardiac myocytes. *Methods Mol Biol.* 2011;689(205-14.
92. Wu Y, Gao Z, Chen B, Koval OM, Singh MV, Guan X, Hund TJ, Kutschke W, Sarma S, Grumbach IM, et al. Calmodulin kinase II is required for fight or flight sinoatrial node physiology. *Proc Natl Acad Sci U S A.* 2009;106(14):5972-7.

Supplementary Tables

Supplementary Table 1. Cardiac morphometric measures and serum chemistry of WT Ctrl and T1D mice at electrophysiology study.

	WT Ctrl	WT T1D
Heart weight/tibial length (mg/mm)	6.85 ± 0.18, n=6	4.93 ± 0.15, n=9****
Atrial weight/tibial length (mg/mm)	0.53 ± 0.03, n=6	0.38 ± 0.02, n=9***
Ventricular weight/tibial length (mg/mm)	6.18 ± 0.20, n=6	4.43 ± 0.15, n=9****
CO_2	15.5 ± 1.1	16.8 ± 0.7
BUN (mg/dl)	24.6 ± 0.7	24.2 ± 1.7
Cr (mg/dl)	0.4 ± 0	0.4 ± 0.03
Serum blood glucose (mg/dl)	183.4 ± 13.4	697.4 ± 48.42****

Heart weight normalized to tibial length (****$p < 0.0001$), atrial weight normalized to tibial length (***$p = 0.0006$,), and ventricular weight normalized to tibial length (****$p < 0.0001$); n = 6 – 9/group. Serum pCO2, BUN, creatinine and blood glucose. (***$p < 0.0001$, n = 4 – 5/group). Data are means ± s.e.m

Supplemental Table 2. Patient characteristics for atrial samples.

Patient Characteristics	**Sinus rhythm and no DM (n = 5)**
Age (year)	68 ± 4
Male:Female	2:3
Ejection Fraction (%)	57 ± 9
Drug Treatment	
B-blocker, n (%)	4/5 (80)
ACEI/ARB, n (%)	5/5 (100)
Calcium channel blocker, n (%)	0/5 (0)
Statin, n (%)	5/5 (100)

ACEI, Angiotensin converting enzyme inhibitor; ARB – Angiotensin receptor blocker.

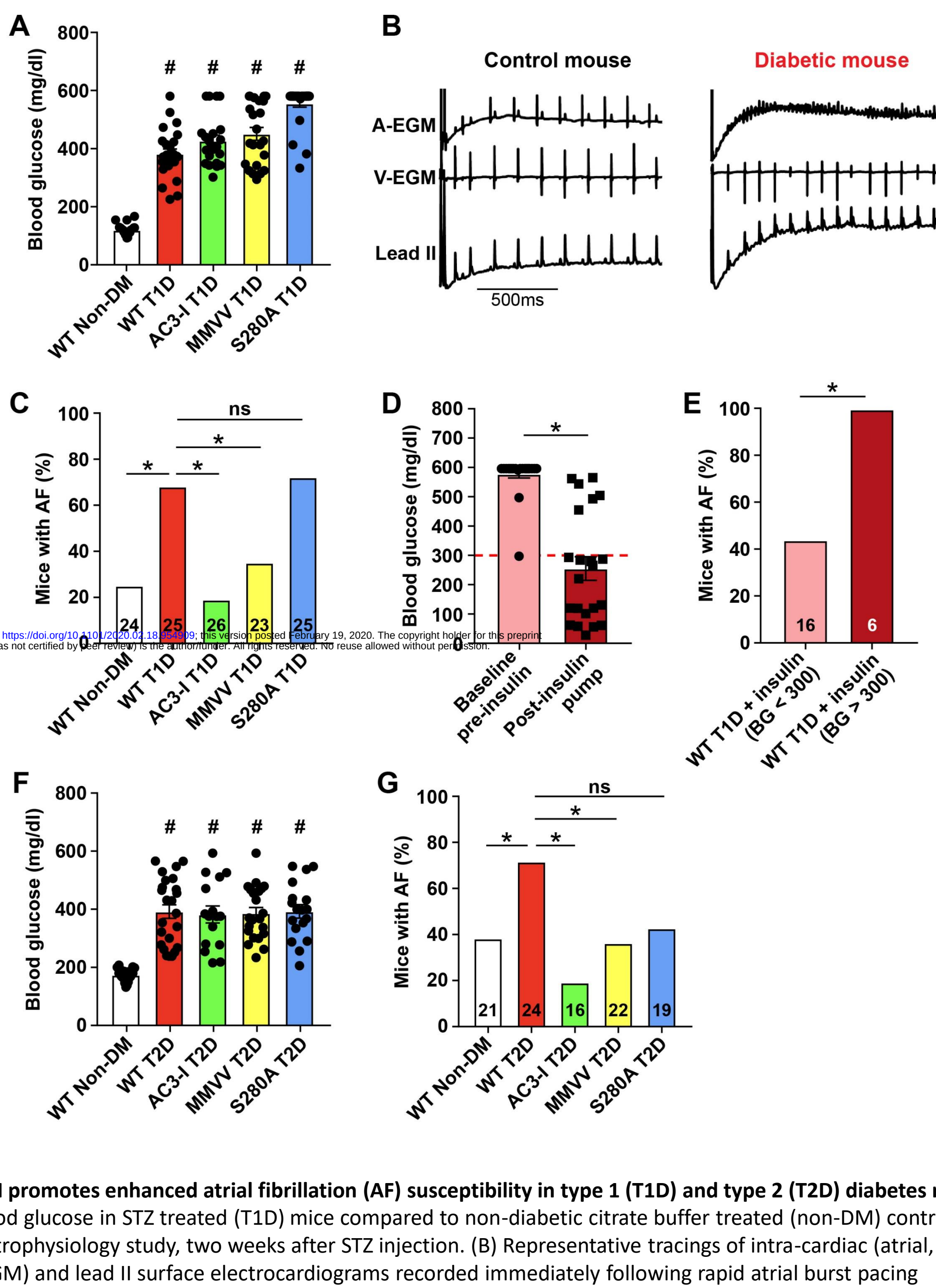

Figure 1. CaMKII promotes enhanced atrial fibrillation (AF) susceptibility in type 1 (T1D) and type 2 (T2D) diabetes mellitus. (A) Elevated blood glucose in STZ treated (T1D) mice compared to non-diabetic citrate buffer treated (non-DM) control mice at the time of electrophysiology study, two weeks after STZ injection. (B) Representative tracings of intra-cardiac (atrial, A-EGM; ventricular, V-EGM) and lead II surface electrocardiograms recorded immediately following rapid atrial burst pacing demonstrating normal sinus rhythm in a control non-DM wild type (WT) mouse and irregularly irregular atrial and ventricular electrical impulses marking AF in a diabetic WT T1D mouse. (C) Marked AF susceptibility in WT T1D mice compared to WT non-DM mice. This is reversed in AC3-I and MMVV T1D mice, but not in S280A T1D mice. (D) Pre- and post-insulin pump (LinBit) implantation blood glucose levels one week after STZ treatment (pre-insulin) and one week after insulin pump implantation (post-insulin). (E) Insulin treatment prevents enhanced AF in WT T1D mice with blood glucose (BG) level less than 300mg/dl on insulin treatment. (F) Elevated blood glucose in T2D mice compared to non-diabetic controls for T2D at the time of electrophysiology study, two weeks after STZ injection. (G) Marked AF susceptibility to AF in WT T2D mice compared to non-diabetic controls. AC3-I and MMVV T2D mice are protected from enhanced AF and there is a trend towards protection in S280A T2D mice ($p = 0.07$). EGM, electrogram; ns, non-significant. Data are represented as mean ± s.e.m, unless otherwise noted. The numerals in the bars represent the sample size in each group. Statistical comparisons were performed using two-tailed Student's t test or one way AVOVA with Tukey's multiple comparison's test for continuous variables and Fischer's exact test for dichotomous variables. (#$p < 0.0001$ versus WT non-DM, *$p < 0.05$).

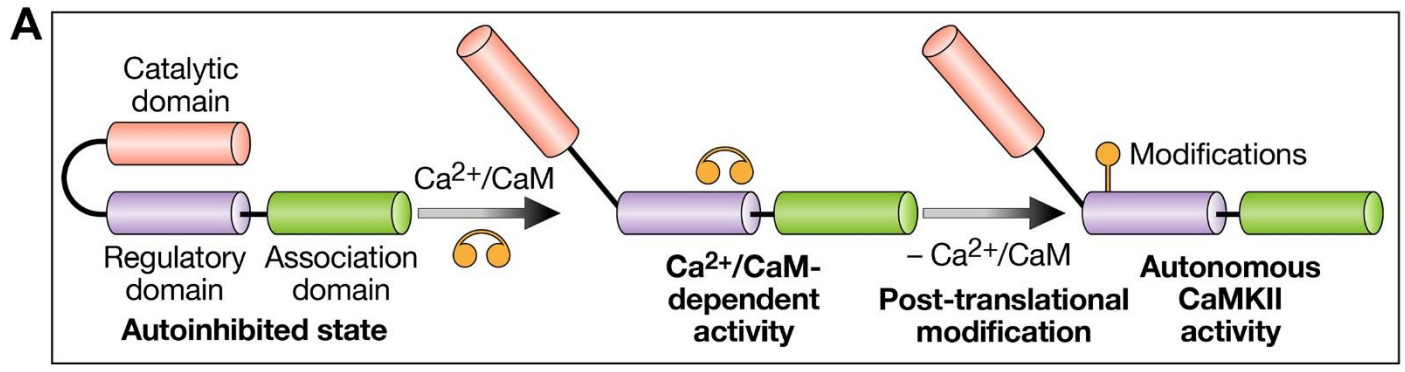

Figure 2. Reactive oxygen species (ROS) and *O*-GlcNAcylation (OGN), upstream activating signals for CaMKII, are elevated in T1D and T2D atria.

(A) Diagram of the CaMKII monomer, consisting of catalytic, regulatory and association domains. Under resting conditions (left panel), CaMKII is inactive because the autoinhibitory region of the regulatory domain (purple segment) constrains the catalytic domain (orange segment). CaMKII activation is initiated by binding of calcified calmodulin (Ca^{2+}/CaM), represented by the orange dumb-bells, to the CaM binding region (middle panel). Post-translational modification of the autoinhibitory region of the regulatory domain 'locks' CaMKII in a constitutively active conformation that persists even after Ca^{2+}/CaM unbinding (right panel). (B) Oxidation at methionines 281/282 and OGN at serine 280 are key post-translational modifications hypothesized to contribute to diabetic heart disease and arrhythmias. (C) Representative confocal images (original magnification, x40) and summary data for DHE fluorescence in mouse atrial tissue show increased ROS in T1D (top panel) and T2D (bottom panel). Scale bars 10µm. (n = 6 WT non-DM, n = 8 WT T1D, n = 4 WT non-DM, n = 4 WT T2D). (D) Representative western blot, Coomassie-stained gels, and summary data for total OGN modified protein levels from atrial lysates from T1D (left panel) and T2D (right panel) (n = 3 – 7/group). (E) Representative western blot for total CaMKII and GAPDH in atrial lysates from WT non-DM, WT T1D, MMVV T1D, S280A WT T1D and S280A T1D. DHE, dihydroethidium; MFI, mean fluorescent intensity. Data are represented as mean ± s.e.m. (*$p < 0.05$).

Figure 3. OGN modulates AF susceptibility in T1D and T2D.
(A) OGN inhibition with DON pretreatment (5mg/kg i.p.) protected from AF in T1D WT and S280A mice, with no additional protection in T1D MMVV mice. (B) DON pretreatment did not protect from AF in T2D WT mice. (C) Schematic of the OGA transgene construct with α-myosin heavy chain (α-MHC) promoter, HA epitope marker and human growth hormone polyA signal (HGH1) (upper panel). PCR product validation of OGA transgene expression in 2 founder pups. The line with the higher OGA expression was chosen for further experiments (lower panel). (D) Western blot for OGA transgene and HA epitope expression in heart, gastrocnemius muscle, liver and kidney from WT and OGA TG mice. (E) OGA TG mice were protected from enhanced AF in T1D. (F) OGA TG mice had similar blood glucose levels as WT littermates under T1D diabetic and non-diabetic conditions. (G) OGA TG were protected from enhanced AF in T2D. (H) OGA TG mice had similar blood glucose levels as WT T2D mice. DON, diazo-5-oxonorleucine. Data are represented as mean ± s.e.m, unless otherwise noted. The numerals in the bars represent the sample size in each group. (*p <0.05).

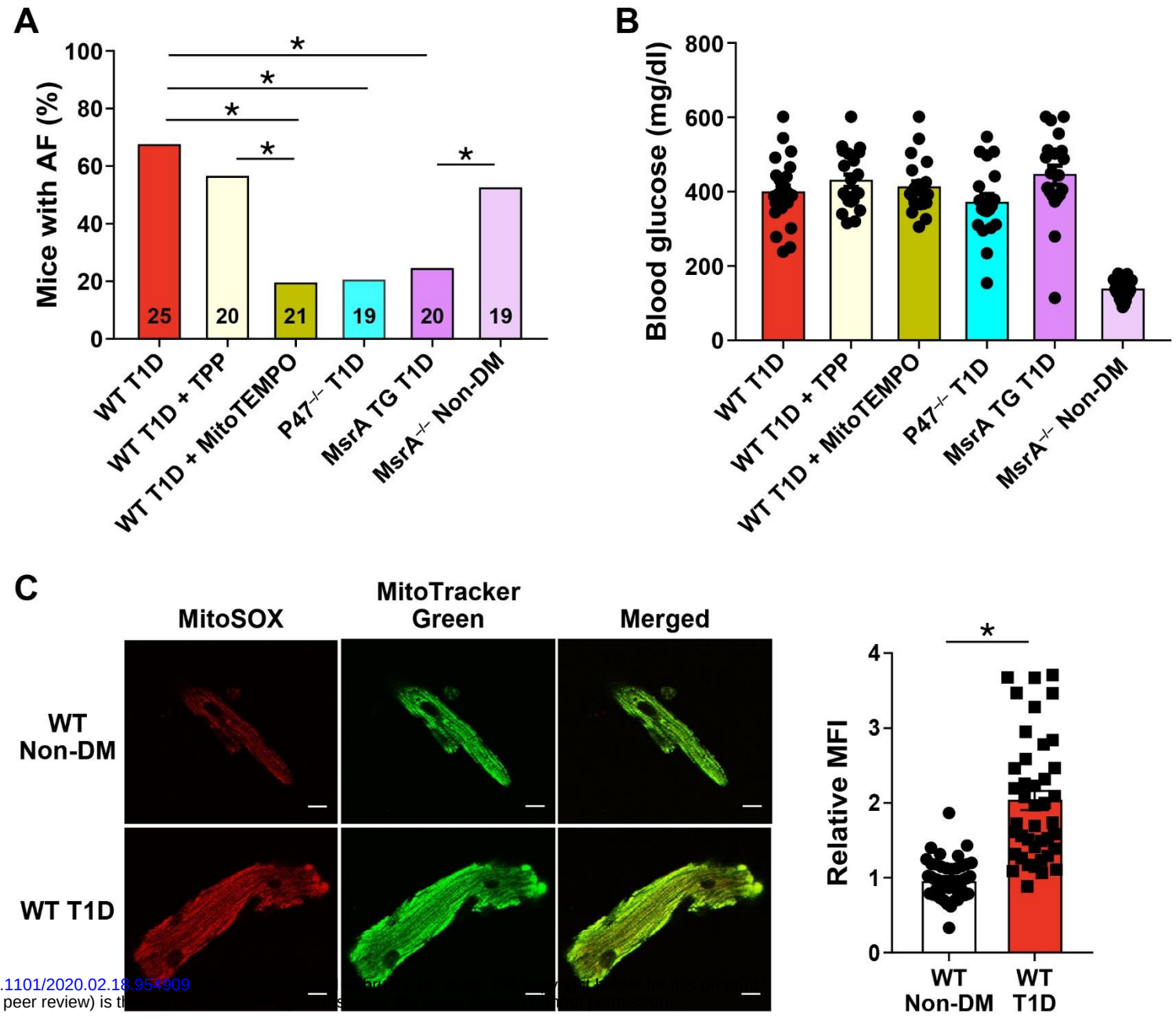

Figure 4. Mitochondrial targeted ROS inhibition protects from AF in diabetes.
(A) Inhibition of mitochondrial ROS by MitoTEMPO treatment, or inhibition of cytoplasmic ROS by loss of the p47 subunit of NADPH oxidase (*p47*$^{-/-}$ mice) protect against AF in T1D mice. Myocardial targeted transgenic overexpression of methionine sulfoxide reductase A (MsrA TG) mice protected from T1D primed AF, while non-diabetic mice lacking MsrA (*MrsA*$^{-/-}$ non-DM) showed increased AF susceptibility in the absence of diabetes. (B) Summary data of blood glucose measurements at the time of electrophysiology study. (C) Increased mitochondrial ROS in isolated atrial myocytes from WT T1D (lower panel) compared to WT non-DM (upper panel) mice detected by MitoSOX fluorescence. Representative confocal fluorescent images (original magnificent, x40) show MitoSOX (red, left), MitoTracker Green (green, middle) and merged images (right). Scale bars 10µm. (n = 41 – 47 cells in each group from 2 mice per group). (D) Representative images of delayed after depolarizations (DADs) and spontaneous action potentials (sAP) in response to rapid pacing in isolated atrial myocytes. (E) Summary data for combined frequency of DADs and sAPs in response to rapid pacing of isolated atrial myocytes (n = 4 – 7 mice/group). Data are means ± s.e.m. Numbers show total number of cells studied per group. (*$p < 0.05$).

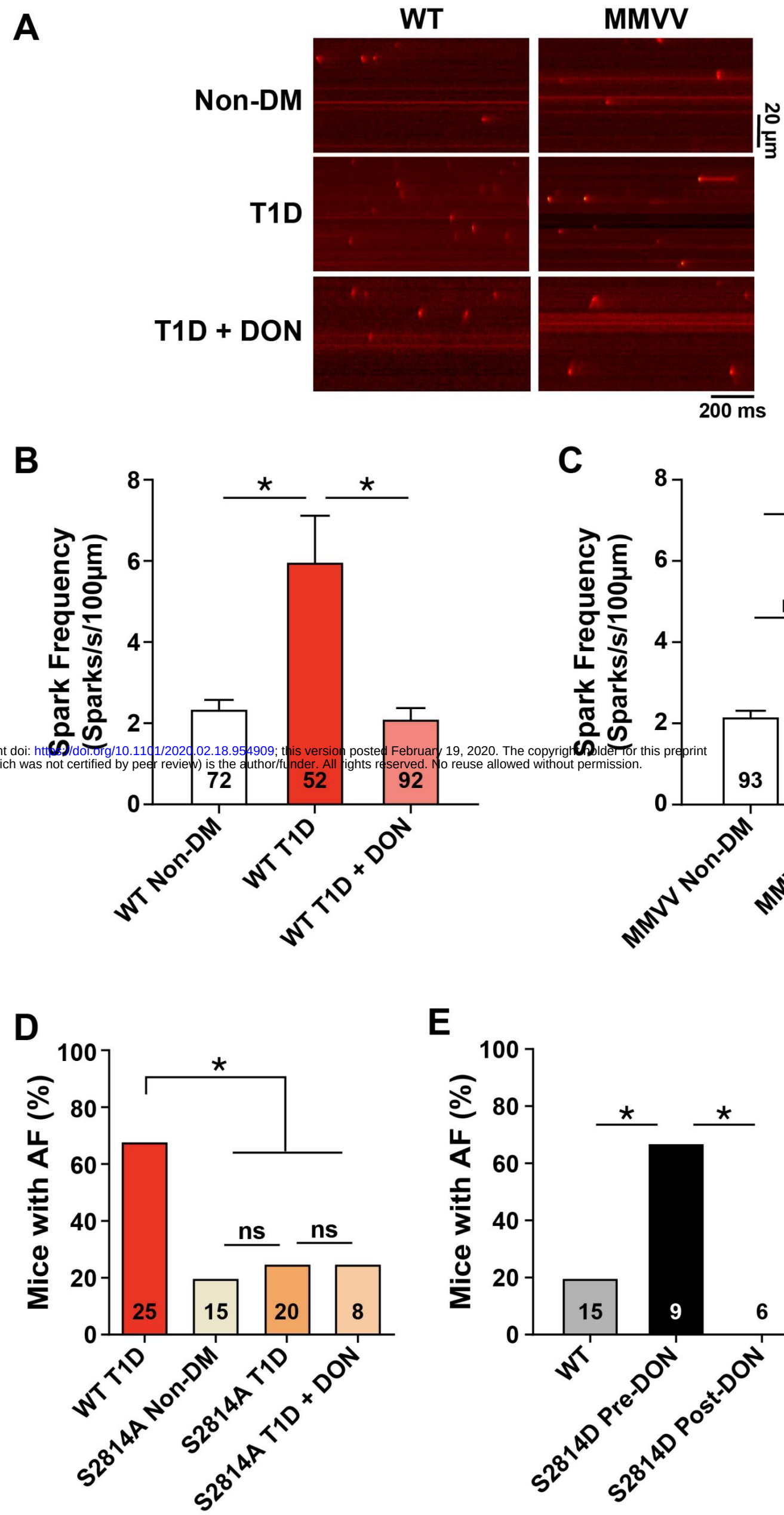

Figure 5. Ox-CaMKII and OGN independently enhance RyR2 Ca^{2+} leak to promote AF in diabetes.
(A) Representative confocal images of Ca^{2+} sparks in atrial myocytes from non-diabetic (non-DM), T1D diabetic and DON pretreated T1D diabetic WT and MMVV mice. Summary data for Ca^{2+} sparks in atrial myocytes from non-DM, T1D and DON pretreated T1D (B) WT and (C) MMVV mice. (n = 52 – 93 cells in each group from 5 – 7 mice/group). (D) S2814A T1D mice and DON pretreated S2814A T1D mice were similarly protected from AF. (E) Summary data of AF incidence in non-diabetic WT, S2814D at baseline (S2814D pre-DON) and S2814D mice treated with DON (S2814D post-DON) after initial AF inducibility at baseline. DON prevented AF in S2814D mice. (F) Summary data for combined frequency of DADs and sAPs in response to rapid pacing of isolated atrial myocytes from S2814D and S2814D mice treated with DON (n = 3 mice/group). Numbers show total number of cells studied per group. Data are means ± s.e.m. (*$p < 0.05$). The numerals in the bars in D and E represent the sample size in each group.

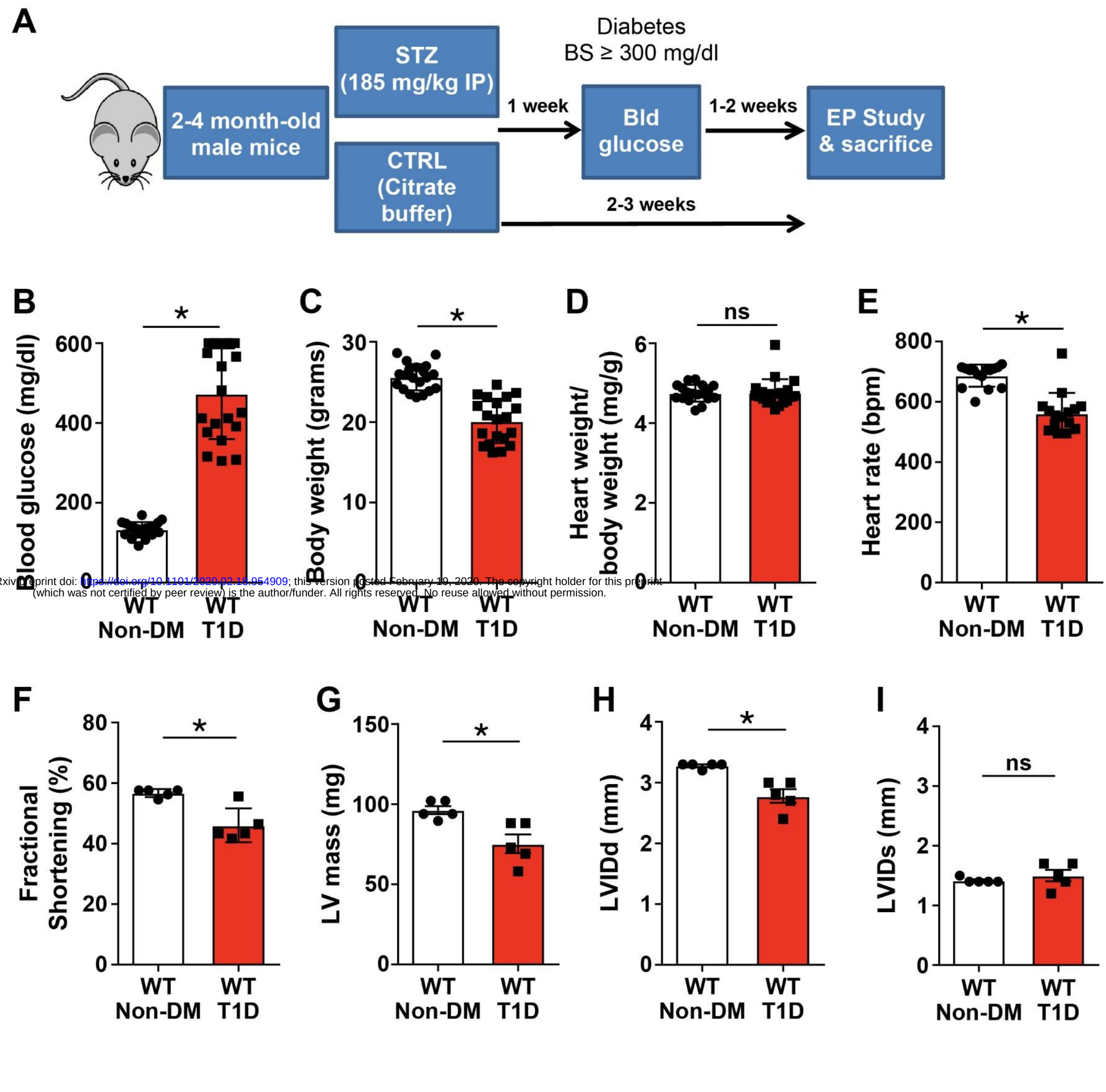

Figure S1. T1D mouse model

(A) Schematic diagram of the protocol for T1D induction and study protocol. Summary data for (B) blood glucose and (C) body weight one week after STZ injection (n = 20 WT non-DM, n = 20 WT T1D). Summary data for heart weight indexed for (D) body weight and (E) heart rate two weeks after STZ injection (n = 18 WT non-DM, n = 20 WT T1D). Summary data of echocardiographic parameters two weeks after STZ injection – fractional shortening (F), LV mass (G), LVIDd (H) and LVIDs (I) in WT non-DM (n = 5) and WT T1D (n = 5). CTRL, citrate buffer; EP, electrophysiology study; LV, left ventricular; LVIDd, LV internal diameter end diastole; LVIDs, LV internal diameter end systole; STZ, streptozocin. Data are represented as mean ± s.e.m., significance was determined using two-tailed Student's t test. (*$p < 0.05$).

Figure S2. T2D mouse model

(A) Schematic diagram of the protocol for T2D induction and study protocol. Summary data of body weight trend (B, left panel) after five weeks of high-fat diet (HFD) and subsequent daily doses of low dose STZ for 3 consecutive days (n = 7 WT non-DM, n = 20 WT T2D); and body weight (B, right panel) and blood glucose (C) two weeks of after STZ injection at time of EP study (n = 21 WT non-DM, n = 24 WT T2D). T2D mice had features consistent with T2D as determined by homeostatic model assessment of insulin resistance, HOMA-IR (D), glucose tolerance test (E) and insulin tolerance test (F) (n = 9 WT non-DM, n = 10 WT T2D). AUC, area under the curve; GTT, glucose tolerance test; ITT, insulin tolerance test. Data are represented as mean ± s.e.m., significance was determined using two-tailed t test. (*p < 0.05).

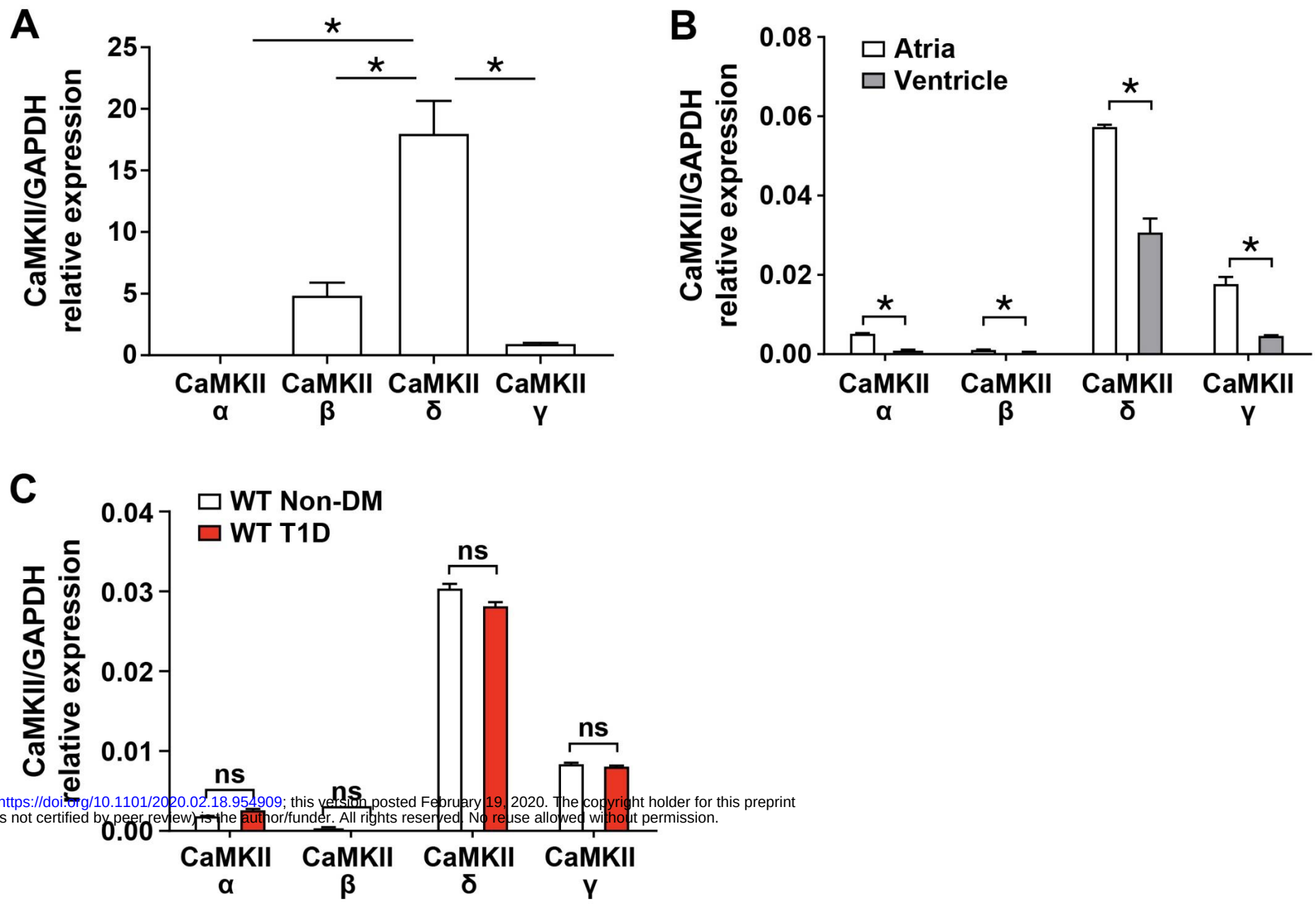

Figure S3. CaMKIIδ is the predominant isoform in mouse and human atria.
(A) CaMKII isoforms (α, β, γ, δ) mRNA expression in human atria from non-diabetic patients with no history of AF measured by qRT-PCR using total RNA (n = 5). See supplemental table 2 for patient characteristics. (B) CaMKII isoforms (α, β, γ, δ) mRNA expression in atria and ventricles from WT non-diabetic mice measured by qRT-PCR using total RNA (n = 5). (C) CaMKII mRNA expression in atria from non-diabetic and T1D WT mice (n = 5 WT non-DM, n = 5 WT T1D). Statistical comparisons were performed using one way AVOVA with Tukey's multiple comparison's post-hoc test. (*$p < 0.05$).

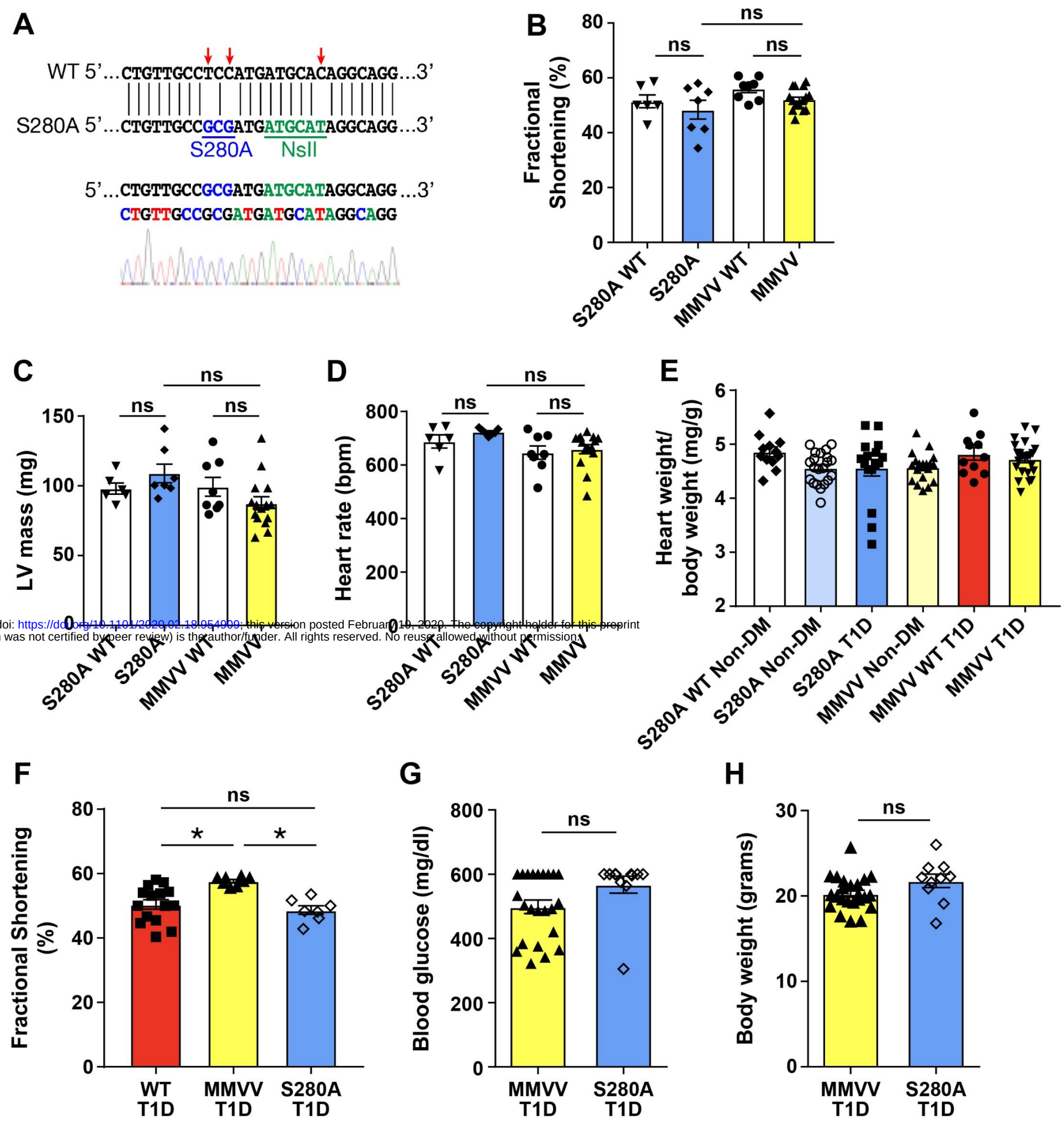

Figure S4. Characteristics of S280A and MMVV mice.

(A) Design of knock-in sequence and Nsil genotyping site for S280A mice (upper panel). F2 sequence showing homozygous S280A (lower panel) No indels present (not shown) (B) Summary data of echocardiographic analysis of non-diabetic S280A and MMVV mice revealed no difference in fractional shortening (B), LV mass (C) or heart rate (D) compared to WT littermates (n = 6 S280A WT, n = 7 S280A, n = 8 MMVV WT, n = 15 MMVV). (E) Summary data for heart weight indexed for body weight in non-diabetic and T1D S280A and MMVV mice and WT littermate controls (n = 12 S280A WT non-DM, n = 21 S280A non-DM, n = 16 S280A T1D, n = 19 MMVV non-DM, n = 11 MMVV WT T1D, n = 23 MMVV T1D). (F) Summary data for left ventricluar fractional shortening in T1D WT, MMVV and S280A mice. MMVV mice were protected from diabetic cardiomyopathy compared to T1D WT and MMVV mice (n = 23 MMVV T1D, n = 11 S280A T1D). Summary data for blood glucose (G) and body weight (H) in T1D MMVV and S280A mice (n = 23 MMVV T1D, n = 10 S280A T1D). Data are represented as mean ± s.e.m., statistical comparisons were performed using two-tailed Student's t test or one way AVOVA with Tukey's multiple comparison's test. (*p <0.05).

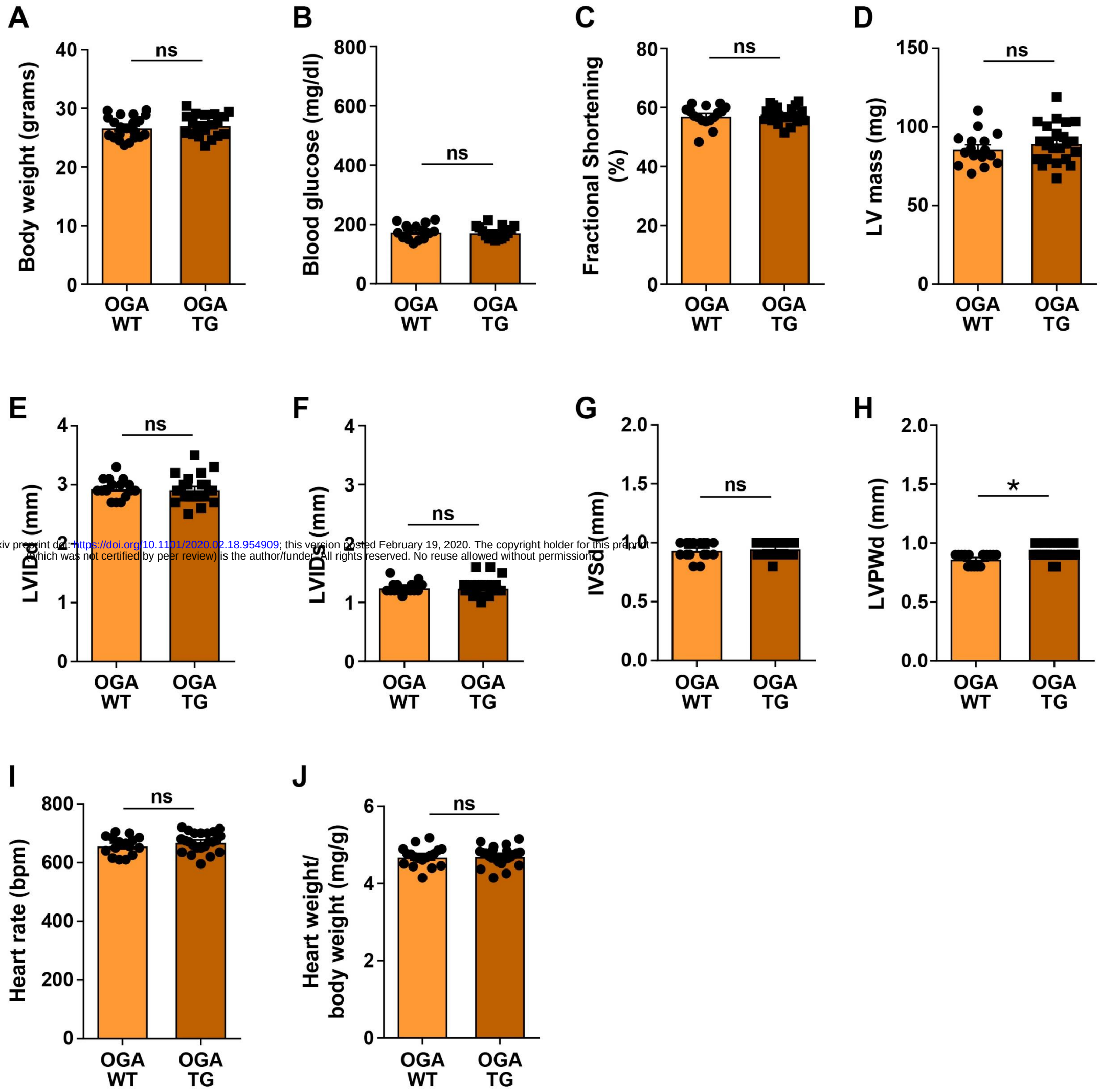

Figure S5. Cardiac phenotyping of OGA TG mice.

(A) Summary data for body weight in WT (n = 21) and OGA TG (n = 19) mice. (B) Summary data for baseline blood glucose in non-diabetic WT (n = 15) and OGA TG (n = 15) mice. Summary data of echocardiographic parameters in non-diabetic WT (n = 16) and OGA TG (n = 23) mice – LV fractional shortening (C), LV mass (D), LVIDd (E), LVIDs (F), IVSd (G), LVPWd (H) and heart rate (I). There were no differences in any of these parameters. (J) Summary data for heart weight indexed for body weight in WT (n = 18) and OGA TG (n = 24). IVSd, interventricular septal end diastolic dimension; LVPWd, left ventricular posterior wall end diastolic dimension. Data are represented as mean ± s.e.m., statistical comparisons were performed using two-tailed Student's t test. (*p <0.05).